OFFSHORE WIND FARMS INTEGRATION USING HVDC TRANSMISSION SYSTEM

Thesis submitted in partial fulfillment of the requirements for the award of degree of

Master of Engineering
in
Power Systems & Electric Drives

Thapar University, Patiala

By:
Neha Singla
(Regn. No. 800941027)

Under the supervision of:
Dr. Sanjay Kumar Jain
Associate Professor, EIED

JULY 2011

ELECTRICAL & INSTRUMENTATION ENGINEERING DEPARTMENT
THAPAR UNIVERSITY
PATIALA – 147004

CERTIFICATE

I hereby certify that the work which is being presented in this thesis entitled "Offshore Wind Farms Integration using HVDC Transmission System" in partial fulfillment of the requirement for the award of the degree of Master of Engineering in Power Systems & Electric drives submitted in Electrical & Instrumentation Engineering Department of Thapar University, Patiala, is an authentic record of my own work carried out under supervision of Dr. Sanjay Kumar Jain, Associate Professor, EIED.

The matter presented in this thesis has not been submitted the award of any other degree of this or any other university.

Neha Singla.
(Neha Singla)

It is certified that the above statement made by the student is correct to the best of our knowledge and belief.

Sanjay 11/07/2011
Dr. Sanjay Kumar Jain
Associate Professor, EIED
Thapar University, Patiala

S. Ghosh 12/7/11
Dr.Smarajit Ghosh
Head of Department, EIED
Thapar University
Patiala

Dr. S. K. Mohapatra
Dean of Academic Affairs
Thapar University
Patiala

ACKNOWLEDGEMENT

I would like to express my gratitude to **Dr. Sanjay Kumar Jain**, Associate Professor, Electrical and Instrumentation Engineering Department, Thapar University, Patiala for his patient guidance and support throughout this thesis work. I am truly very fortunate to have the opportunity to work with him. He has provided me help in technical writing and presentation style, and I found this guidance to be extremely valuable.

I am very thankful to Head of the Department, **Dr. Smarajit Ghosh**, for his encouragement, support and providing the facilities for the completion of this thesis.

I am also thankful to entire faculty and staff members of Electrical and Instrumentation Engineering Department for their unyielding encouragement.

I am greatly indebted to all my friends, who have graciously applied themselves to the task of helping me with ample morale support and valuable suggestions. Finally, I would like to extend my gratitude to all those persons who directly or indirectly helped me in the process and contributed towards this work.

Neha Singla.

Neha Singla

ABSTRACT

Human efforts of harnessing wind energy had started in ancient times, when they used to sail ships and boats. Wind has gained popularity mainly in recent years, as it is renewable, eco-friendly, non-polluting and non-depleting source of energy.

Wind parks are planned to be placed into sea far away from the mainland. The wind speed does not remain constant and thus require a generation which can extract maximum power from the wind. Doubly fed Induction Generator (DFIG) is a solution for such large wind turbines connected with offshore wind farms. The stator of the generator is directly connected to the grid while the rotor is connected through back-to back converter. With this the maximum power from the DFIG can be harnessed.

The modeling and dynamic performance of the wind driven DFIG system is studied for two cases: DFIG Connected with AC system and DFIG connected with HVDC system. The system model is realized in simulink environment. The performance of system is investigated for the change in wind speed, change in grid voltage, change in load and change in length of the transmission line for AC and HVDC systems.

TABLE OF CONTENTS

LIST OF FIGURES

NOMENCLATURE

p is the derivative symbol

V_{qs} ,V_{ds} are the three-Phase supply voltages in d-q reference frame, respectively

i_{qs} ,i_{ds} are the three-Phase stator currents in d-q reference frame, respectively

φ_{qs} ,φ_{ds} are the three-Phase stator flux linkages in d-q reference frame, respectively

V_{qr} ,V_{dr} are the three-Phase rotor voltages in d-q reference frame, respectively

i_{qr} , i_{dr} are the three-Phase rotor voltages in d-q reference frame, respectively

φ_{qr} ,φ_{dr} are the three-Phase rotor voltages in d-q reference frame, respectively

r_s ,r_r are the stator and rotor resistances of machine per phase, respectively

L_{ls}, L_{lr} are the leakage inductances of stator and rotor windings, respectively

ω_e ,ω_r are the supply and rotor angular frequency (electrical speed), respectively

θs ,θr are the stator and rotor flux angle, respectively

T_e ,T_m are the electromagnetic and mechanical torques, respectively

P_s ,Q_s are the stator-side active and reactive powers, respectively

P_r ,Q_r are the rotor-side active and reactive powers, respectively

D, J are the moment of inertia and damping coefficient, respectively

P is the Number of poles

M_1,M_2 is the stator and rotor modulation depths, respectively

V_{tri} is the triangular Voltage Signal

R,L are the resistance and inductance of input filter, respectively

V_1, I_1 are the input filter line voltage and current, respectively

E is the DC-link voltage

C is the DC-Link capacitance

P_{DC} is the DC-link active power

σ is the leakage factor

k_p ,k_i are the proportional and integral gain, respectively

α is the bandwidth of the closed-loop system

α_{cs} is the Bandwidth of supply-side current controller

α_E is the bandwidth of DC-link voltage controller

α_{cr} is the bandwidth of rotor-side current controller

α_ω is the bandwidth of speed controller

comp stands for compensation term

e identifies synchronously rotating reference frame

CHAPTER 1
INTRODUCTION

1.1 OVERVIEW

Wind energy has gained popularity in recent years all over the world, mainly because wind energy is renewable and eco-friendly. There are, however, many challenges associated with harnessing this type of energy for grid application mostly due to its intermittent nature.

Wind is a result of the sun shining unevenly on the earth. The corresponding daily and seasonal changes in temperature consistently generate wind, producing a fuel source that can never be depleted. Wind turbines convert the kinetic energy in the wind into mechanical power. This mechanical power can be used for specific tasks (such as grinding grain or pumping water) or a generator can convert this mechanical power into electricity to power homes.

Human efforts to utilize wind for energy have started in ancient times, when they used to sail the ships and boats. Later wind energy served the mankind by providing the energy for grinding mills and water pumps. During its transformation from these crude and heavy devices to today's efficient and sophisticated machines, the technology went through various phases of development. In Holland, several decisive improvements were made on wind mills in the 16th century, leading to new types of mill, so called Dutch wind mill. The era of wind electric generators began close to 1900's. The first modern wind turbine, specifically designed for electricity generation was constructed in Denmark in 1890. The wind electric generators became commercially available in American market by 1925. However at that time the electricity generated from wind was costing 8-10 times more than that from fossil fuels. But oil crisis in 1970's forced the world to think about wind power generation and to work for cost efficient measures. Wind power, which has been proved as a potential source for generation of electricity with minimal environmental impact, is the fastest growing source for electric power generation and it is expected to remain so in future. Countries like Germany, United States of America, China and India have taken a lead in harnessing this nonpolluting and replenishable source of energy.

Harnessing wind energy for electric power generation is an area of research interest and at present, the emphasis is given to the cost effective utilization of energy resource for quality and reliable power supply. Among various techniques, the use of the doubly fed induction generator appeared to be a good solution for such applications. The induction generated is favored for wind power plants because of its simplicity, robustness and small size per generated kW, lower maintenance and ease of control.

For, wind generation either fixed speed or variable speed turbines can be used. These turbines are classified into four major types by the Western Electricity Coordinating Council (WECC) to develop standard wind turbine models. These types are:-

Type I Pitch regulated squirrel cage induction generator directly coupled to the grid.

Type II Variable slip squirrel cage induction generator directly coupled to the grid.

Type III Wound rotor induction generator with an AC/DC/AC power converter connected between the rotor terminals and grid and is pitch regulated.

Type IV Synchronous or asynchronous machine connected to the grid using full rated AC/DC/AC power converter and is pitch regulated.

The Type I and Type II use the simplest topology where the turbine is directly connected to the grid. Machine needs a switch to prevent motoring operation during low wind speeds and also suffers a major drawback of reactive power burden on the grids as there is no reactive power control. Type II uses an electronically modulated rotor resistance to effect dynamic changes in the machine torque speed characteristics.

The Type III is the most common for high power grid applications. This topology allows the complete control of reactive power using rotor and grid side converters. The converters used for this topology need to be rated at only 25% to 30% of overall machine rating as they are used on the rotor side to supply the slip power which is not exceeding to 25% to 30% of the overall machine power.

The Type IV topology uses a full rated converter with either a synchronous or an asynchronous machine. This topology has full control of the reactive power and speed. The major advantages associated with Type III wind turbines are that it has four quadrant

active and reactive power flow capabilities. With constant frequency power output and low power converter ratings, it the most widely used topology. Hence this dissertation focuses attention on the integration of Doubly Fed Induction Generator (DFIG) – Type III based wind turbines to the power grid.

Wind parks of thousands of MW are planned to be placed into sea far away from the mainland. Appropriate transmission systems should be designed to handle such significant amount of power, which is resulting high efficiency while is economically competitive.

The use of classical HVDC converter based on thyristor valves, although resulting into low losses, is not the best solution when it comes to offshore wind farms because it requires large converter station for both, the onshore and the offshore side. The HVDC converter are further not suited for offshore application because it needs an auxiliary service at the offshore converter station for the operation of the line-commutated converters during power failures; it is essential to have an AC voltage source for commutation and to facilitate the power transfer between two AC networks; offshore grid needs power before the start of wind farms, no independent control of the active and reactive power. The voltage source converter (VSC) based HVDC system uses high switching frequency transistors like IGBTs. The IGBTs are having self-commutated turn-on and turn-off capability and therefore, allowing the generation of reactive power to supply the wind turbines. Further, this configuration voltage and power control. The voltage and reactive power control are vital for stability of the system. Therefore, VSC-HVDC can be suited for connecting a large offshore Wind Farm to the shore point.

For such applications, the HVDC transmission is suited instead of AC transmission because of low losses for long distances, lower cost for cables above certain distances, ability to connect asynchronous AC networks, ability to operate at variable speeds, decoupling of the connected AC networks etc.

1.2 LITERATURE REVIEW

Doubly fed induction generators (DFIGs) are an economic variable-speed solution for large wind turbines whereas HVDC transmission is being considered for the grid connection of some offshore wind farms. The need for coordination control of the DFIG

and the HVDC link, based on conventional thyristor has been analyzed [1-3]. It has been emphasized that the individual generator should be controlled for power tracking in a way similar their control during direct connection to an ac grid.

High voltage DC transmission using voltage source converters facilitate variable frequency operation in the wind farm grid. Variable frequency operation reduces the machine slip. Thus, a lower rated converter is sufficient for the same speed range. The variable frequency operation of doubly-fed induction generators have been presented in [4-6] in which the performance has been evaluated under MATLAB/Simulink environment.

The turbine modeling has been used to extract maximum possible mechanical power from the wind according to the wind velocity and tip-speed ratio. The DFIG model based on the vectorized dynamic approach has been presented in [7-10]. The presented model can be applicable for all types of induction generator configurations for steady state and transient analysis.

Voltage control for large quantities of wind turbines suddenly drawn out of the grid, power factor control, with the wind turbine of low voltage crossing, branch short circuit fault is taken into full consideration in all these cases. It has been suggested in papers [11-13] that the transient stability of DFIG connected to power system is better than that of synchronous generation units.

A dynamic model with reduced-order double cage representation for the DFIG and its associated control and protection circuits are taken into consideration [14]. It has been demonstrated that by properly selecting the proportional gain of the speed and power factor controller, it is possible to enhance significantly the stability of the DFIG.

The grid-connected wind driven doubly fed induction has been studied [15]. The modeling of the machine for various operating conditions below and above synchronous speed is achieved by means of double sided PWM converter joining the machine rotor to the grid. Stator-flux-oriented vector control approach is applied. Switch by switch representation of PWM converters with a carrier based SPWM modulation for both converters have been proposed [16]. Provides independent control of active and reactive power for both converters and DC link voltage is constant.

The development and performance comparison of a conventional PI controller and a pitch angle controller based on pole-placement theory for DFIG-based Wind Energy Conversion Systems are verified [17]. D-Q reference based mathematical modeling of the DFIG and the controllers have been presented. The Pitch angle controller is however more efficient when wind speed suddenly changes and is more robust under parameters variations of the DFIG.

A DFIG model is compatible with transient analysis which has independent control of torque and reactive power for wind turbines [18]. Wind turbine has been simulated by incorporating aerodynamics and pitch control by assuming that the frequency converter is ideal.

The control dynamics of a DFIG based variable speed wind turbine operating in two modes operation and during transition period are investigated [19]. Mathematical analysis and corresponding modeling results has been presented which show that the power flow in the rotor circuit under different modes can be controlled by changing current and voltage phase sequence through the rotor side converter and line side converter.

The connection of an offshore wind farm depends primarily on its installed power capacity and on distance to the connection point of the system. The advantages of using a HVDC solution are more significant for high power and longer distance [20-21]. An equivalent d-q averaged model is developed for an HVDC-VSC System [22]. The HVDC technology has been proposed as one of the most promising FACTS in future power systems, suitable for transient stability analysis and control design. The performance of controller shows better results than PI controllers, having better stability margin and shorter time response.

1.3 OBJECTIVE OF WORK

The present work has been carried out with the objective to study dynamic performance of wind driven grid connected doubly fed induction generator by formulating appropriate mathematical models. Further, the aim is to study and simulate a long distance HVDC system to transmit the energy generated from wind source for load/grid located at far distant locations.

1.4 ORGANIZATION OF THESIS WORK

The work carried out in this thesis has been summarized in five chapters. The **Chapter 1** summarizes the overview of thesis, brief literature review, objectives of work and organization of the thesis. The **Chapter 2** describes the power from the wind, modeling and control of wind turbine. The **Chapter 3** summarizes the operating principle and modeling of doubly fed induction generator. The **Chapter 4** summarizes the basics of HVDC system along with its modeling. The **Chapter 5** presents the simulation and results obtained from developed simulink models.

CHAPTER 2
WIND: A SOURCE OF ELECTRIC POWER

2.1 INTRODUCTION

Wind energy conversion systems can be classified based on turbines that depend on aerodynamic drag and turbines that depend on aerodynamic lift. Wind power has been used for centuries for different purposes such as: pumping water, propelling boats or grinding corn. The early Persian vertical axis wind turbine utilized the drag principal. The history of wind power shows a general evolution from use of simple light devices driven by aerodynamic drag forces, to heavy, material-intensive drag devices and finally to the use of light material, and efficient aerodynamic lift devices in the modern era. The earliest known use of wind power, such as sail boat form ancient Persia used this technology. The typical drag device based on Persian design is shown in Fig. 2.1. It had a significant impact on the pursuing wind power development.

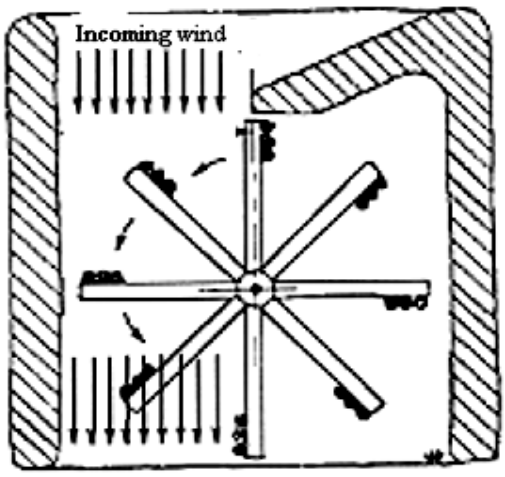

Fig.2.1 Drag device based on Persian design, used in the sail boat

Modern wind turbines are predominately based on aerodynamic lift. Lift devices use blades that interact with incoming wind. The force resulting from the blade (airfoil) interaction with the air flow consists of the drag force component in the direction of the flow and a force component that is perpendicular to the drag, namely the lift. Magnitude of the lift force could be several times larger than drag force depending on the design of the

airfoil blade, which provides the driving force for the rotor. Wind turbine based on aerodynamic lift can be further classified according to the orientation of spin axis, as vertical axis turbine and horizontal axis turbine. The vertical and horizontal axis turbines are shown in Fig. 2.2(a) and Fig. 2.2(b) respectively. In the vertical axis wind turbine, the main rotor shaft is set vertically. The advantages of this arrangement are that generators and gearboxes can be placed close to the ground and these devices do not need to be pointed into the wind direction.

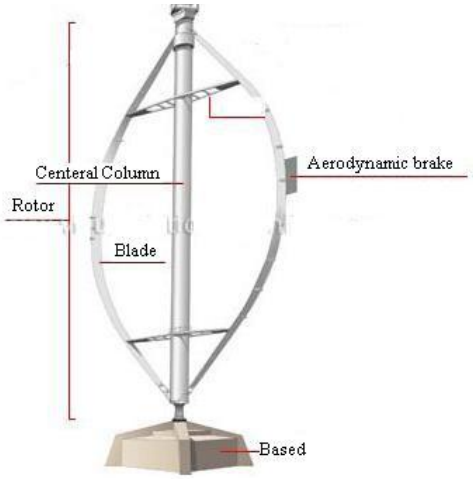

Fig 2.2(a) Vertical Axis wind turbine

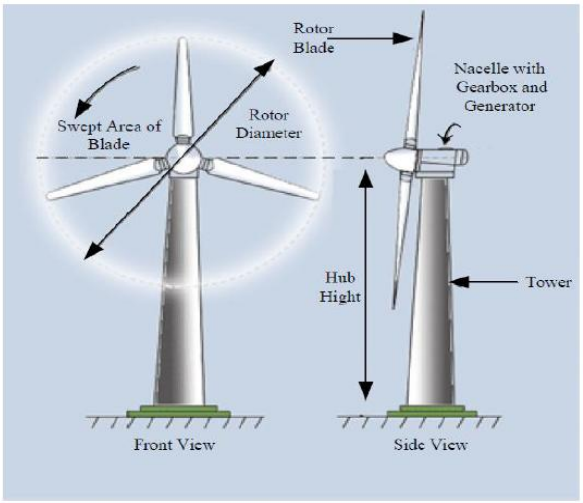

Fig.2.2(b) Horizontal Axis wind turbine

Horizontal axis type of turbine consists of a tower, a nacelle that is mounted on the top of the tower and contains a generator, gearbox and the rotor. Wind turbines extract the energy from the wind by transferring the thrusting force of the air passing through the

turbine rotor into the rotor blades. There are two primary physical principles by which energy can be extracted from the wind; these are through the creation of either drag or lift force (or through a combination of the two). The cross section of rotor wing as shown in Fig 2.3 will help understanding these principles. The wind passes over both surfaces of the airfoil shaped blade. As wind passes more rapidly over the upper side of the airfoil, creating a lower- pressure area above the airfoil. The pressure differential between top and bottom surfaces creates a thrust force, called aerodynamic lift.

In addition to lift force, a drag force perpendicular to the lift force impedes rotor rotation. A prime objective in wind turbine design is for the blade to have a relatively high lift-to-drag ratio. This ratio can be varied along the length of the blade to optimize the turbine's energy output at various wind speeds. In an aircraft wing, this force causes the airfoil to rise, lifting the aircraft off the ground. Since the blades of a wind turbine are constrained to move in a plane with the hub as its center, the lift force causes rotation about the hub. As a result, the lifting force is converted into a mechanical torque and this torque makes the shaft, as part of the turbine rotor, turn. The power in the shaft is used to produce electricity by coupling it with generator.

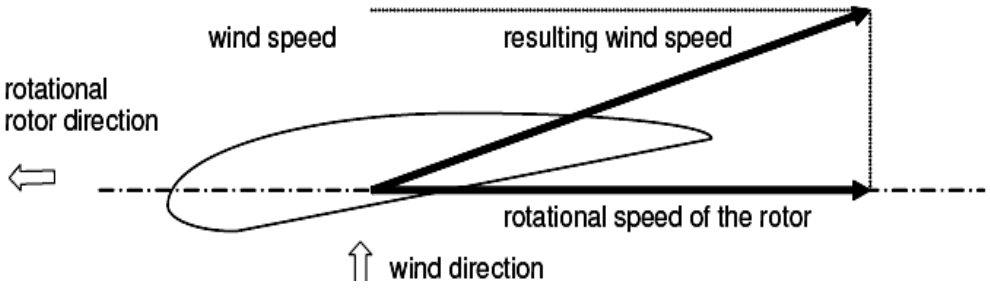

Fig.2.3 Cross section of a rotor wing

The basic features that characterize lift and drag are:

- Drag is in the direction of airflow.
- Lift is perpendicular to the direction of airflow
- Generation of lift always causes a certain amount of drag to be developed
- With a good aerofoil, the lift produced can be thirty times greater than the drag. Lift devices are generally more efficient than drag devices

2.2 POWER FROM WIND

A simplified block diagram of the wind turbine components is presented in Fig. 2.4. As shown in the scheme, the elements of wind turbine are the wind model, the aerodynamic model, the mechanical model, the generator model, the rectifier and the pitch control block model. The input of the system is the wind and the output is the electrical power. The wind model provides a realistic characteristic of the wind which is modeled based on an average wind speed profile. The wind is applied to the rotor blades. The aerodynamic model computes the rotor torque which is the input for the mechanical model that makes the conversion of the mechanical torque of rotor into a torque proper for the high speed shaft.

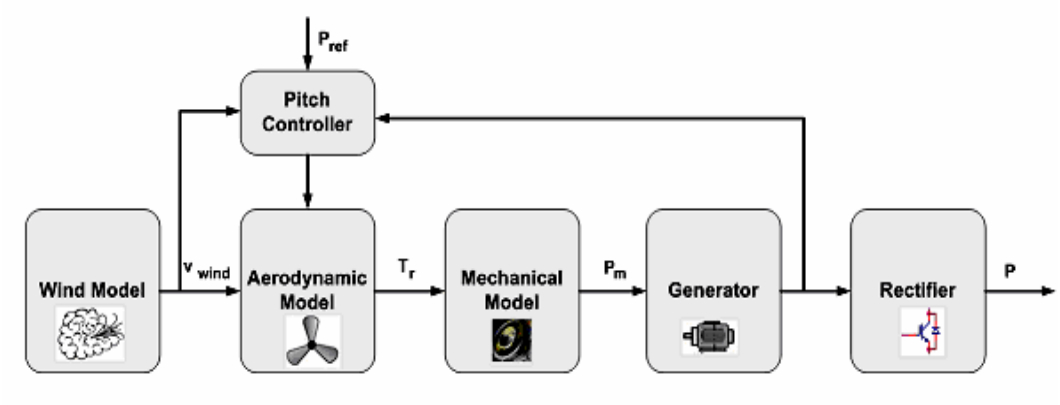

Fig.2.4 Wind Turbine Model

The generator can be a Doubly fed Induction Generator. This performs the conversion of the mechanical power outputted by the mechanical model (Pm) into the electrical power, followed by the transformation from an AC to DC transmission system made by the rectifier.

The aim of the pitch controller is to ensure that the wind turbine, depending on the available wind is producing the desired power. Based on the measured power of the system and the reference value for power, the pitch control has to adjust the angle of the blades in order to maintain a constant reference power when higher winds are applied to the wind turbine. The power reference can be set to be the rated power of the wind turbine but depending on the demands of electricity. The grid operator can change this reference in order to maintain the stability of the grid.

2.3 MODELING OF WIND TURBINE

From a physical point of view, the static characteristics of a wind turbine rotor can be described by the relationships between the total power in the wind and the mechanical power of the wind turbine. These relationships are readily described starting with the incoming wind in the rotor swept area. It can be shown that the kinetic energy of a cylinder of air of radius R travelling at wind speed V_{wind} corresponds to a total wind power P_{wind} within the rotor swept area of the wind turbine. The P_{wind} can be expressed as,

$$P_{wind} = 0.5\rho_{air}\pi R^2 V_{wind}^3 \quad \text{.....(2.1)}$$

Where, ρ_{air} is the air density (1.225 kg/m^3), R is the rotor radius and V_{wind} is the wind speed.

It is not possible to extract all the kinetic energy from the wind since this would mean that the air would stand still directly behind the wind turbine. This would not allow the air to flow away from the wind turbine, and clearly this cannot represent a physical steady-state condition. The wind speed is only reduced by the wind turbine, which thus extracts a fraction of the power in the wind. This fraction is expressed as the power efficiency coefficient, Cp, of the wind turbine. Therefore the mechanical power output of the wind turbine P_{mech} considering the definition of Cp can be stated as given by

$$P_{mech} = C_p P_{wind} \quad \text{.....(2.2)}$$

Therefore, eq. 2.1 can be written as,

$$P_{mech} = 0.5 C_p \rho_{air} \pi R^2 V_{wind}^3 \quad \text{.....(2.3)}$$

It can be shown that the theoretical static upper limit of Cp is approximately 0.59. This suggests that 59% of the maximum kinetic energy can be extracted from the wind. This is known as Betz limit. A modern three bladed wind turbine has an optimal Cp value in the range of 0.52-0.55 when measured at the hub of the turbine.

From a physical point of view the power, P_{mech} that is extracted from the wind will depend on rotational speed, wind speed and blade angle, β. Therefore, P_{mech} and Cp are functions of these parameters.

$$P_{mech} = f(\omega_{turb}, V_{wind}, \beta) \quad \text{.....(2.4)}$$

The forces of the wind on a blade section and thereby the possible energy extraction will depend on the angle of incidence φ between the plane of the moving rotor blades and the relative wind speed V_{rel} as seen from the moving blades. Simple geometrical considerations are shown in Fig. 2.5. The wind turbulence created by the blade tips has been ignored and the angle of incidence φ is determined by the incoming wind speed V_{wind} and the speed of the blade. The blade tip is moving at speed V_{wind}, equal to (ω_{turb}*R). The highest values of Cp are typically obtained for values in the range 8 to 9 (i.e. when the tip of the blade moves 8 to 9 times faster than the incoming wind). This means that the angle between the relative air speed from the blade tip and the rotor plane is rather a sharp angle.

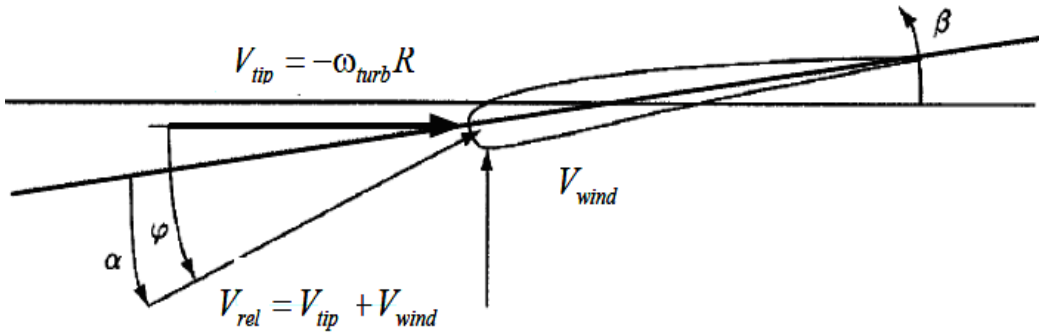

Fig.2.5 Illustration of forces around the moving blade

Where, V_{tip} = tip speed; ω_{turb} = turbine rotational speed; R = rotor radius; V_{rel} = relative wind speed; V_{wind} = wind speed; α = angle of attack; φ = angle of incidence between the plane of the rotor and V_{rel}; β= blade angle.

On modern wind turbines, it is possible to adjust the pitch angle β of the entire blade through a servo mechanism. If the blade is turned, the angle of attack α between the blade and the relative wind V_{rel} will be changed accordingly. Again, it is clear from a physical perspective that the forces of the relative wind on the blade, and thereby the energy extraction, will depend on the angle of attack α between the moving rotor blades and the relative wind speed V_{rel} as seen from the moving blades. Hence Cp can be expressed as a function of λ and β:

$$C_p = f(\lambda, \beta) \quad \text{.....(2.5)}$$

2.4 PITCH AND STALL CONTROL OF WIND TURBINE

An effective control system should be designed to control the output power of wind turbine to maximize their output. In case of stronger winds it becomes necessary to waste part of the excess energy of the wind in order to avoid damaging the wind turbine. The wind turbines are designed to yield maximum output at wind speeds of 12-15 metres per second because the probability of this speed of wind is very high. It is not economical to design turbines that maximize their output at stronger winds because such strong winds are rare. Two types of controls are used. These controls are –

- **Pitch control**
- **Stall control**

The propellers **pitch** needs to be controlled whenever, the average of wind speed changes over a propeller. Commercial wind turbines are designed to produce optimum power with 11 m/s of wind speed. However, the wind speed always fluctuates up and down around this optimum. To generate the optimum power, the turbine blades have to adjust accordingly. This adjustment comes from turning the blades around their longitudinal axis (to pitch). When the wind speed decreases, the blade pitch is adjusted such that it exposes more surface area to the wind. Conversely, when wind speed picks up, the blade pitch is adjusted such that it exposes less surface area to the wind. If a blade is not designed for stall, increased wind speeds will force the rotor to turn faster without a pitch control mechanism. The pitch mechanism allows the wind to flow around the blade as smoothly as possible. To do this, air particles cannot hit the blade head on, rather they must flow almost tangent to the blade just as in an airplane's wing operating in the air.

The **Stall control** of wind turbine works by increasing the angle at which the relative wind strikes the blades (angle of attack), and it reduces the induced drag (drag associated with lift). Stalling increases automatically when the winds speed up. The rotor blade has been aerodynamically designed to ensure that the moment wind speed becomes too high. Stalling creates turbulence on the side of the rotor blade not facing the wind. This stall prevents the lifting force of the rotor blade from acting on the rotor. A rotor blade for a stall controlled wind turbine is twisted slightly along its longitudinal axis. This is partly done in order to ensure that the rotor blade stalls gradually rather than abruptly when the wind speed reaches its critical value. The basic advantage of stall control is that one avoids moving parts in the rotor itself, and a complex control system.

2.5 DRIVERS FOR WIND ENERGY

The growth of the market for wind energy is being driven by a number of factors, including the wider context of energy supply and demand, the rising profile of environmental issues, especially climate change, and the impressive improvements in the technology itself. These factors have combined in many regions of the world to encourage political support for the industry's development. These factors are-

- Global demand for energy is increasing at a breathtaking pace, which will require significant investment in new power generation capacity and grid infrastructure. Just as energy demand continues to soar, supplies of fossil fuels are dwindling and prices are at their most volatile. Wind energy, however, is a massive indigenous power source which is available virtually everywhere in the world. There are no fuel costs, no geo-political risk and no supply dependence on imported fuels from politically unstable regions. Every KWh generated by wind power has the potential to displace fossil fuel imports, improving both **security of supply** and the national balance of payments.

- Wind energy makes sound **economic** sense, in contrast to other generation sources, the price for the fuel needed over the total lifetime of a wind turbine is well known, it is zero. This takes away a substantial part of the investor's risk. At many sites, wind power is already competitive with new-built conventional technologies and in some cases much cheaper. When taking into account the price of carbon, wind power is even more attractive. Job creation and regional economic development are also key factors in economic considerations around wind power. The wind power industry is revitalizing regional economies, providing quality jobs and expanding tax bases in rural regions struggling to keep their economies moving ahead in the face of the global flight to the cities. This is resulting into regional economic development as experienced in Tamil Nadu and Gujarat.

- Wind power is a clean, emissions-free power generation technology. Wind energy is the only power generation technology that can deliver the deep cuts in CO_2 emissions. The world needs to combat the worst effects of climate change; it also provides numerous other **environmental benefits**. It has a positive effect on air pollution as wind energy does not produce any toxic waste. In addition, wind

energy uses virtually no water, which, in an increasingly water stressed world, is a major environmental consideration. The wind energy not only reduces the emission of green house gases it also has a positive effect on the quality of air we breathe.

- Wind energy does not deplete **natural resources**. Unlike fossil fuels that have a finite supply, wind is renewed every day as the earth heats and cools that makes it very attractive. Approximately one pound of coal is saved by every kilowatt-hour generated by wind.

2.6 DIFFICULTIES WITH WIND POWER

Despite of many benefits of wind power, there are some difficulties also in converting the wind energy into electric power these include-

- **Variability of wind power**
- **Grid Connection**

Wind power is often described as an **"intermittent"** energy source, and therefore unreliable. In fact, at power system level, wind energy does not start and stop at irregular intervals, so the term "intermittent" is misleading. The output of aggregated wind capacity is variable, just as the power system itself is inherently variable. Since wind power production is dependent on the wind, the output of a turbine and wind farm varies over time, under the influence of meteorological fluctuations. These variations occur on all time scales: by seconds, minutes, hours, days, months, seasons and years. Understanding and predicting these variations is essential for successfully integrating wind power into the power system and to use it most efficiently. The power systems are influenced by a large number of planned and unplanned factors, but they have been designed to cope effectively with these variations through their configuration, control systems and interconnection.

Technical requirements within **grid codes** vary from system to system, but the typical requirements for generators normally concern tolerance, control of active and reactive power, protective devices and power quality. Specific requirements for wind power generation are changing as penetration increases and as wind power is assuming more and more power plant capabilities, i.e. assuming active control and delivering grid support services. In response to increasing demands from the network operators, for

example to stay connected to the system during a fault event, the most recent wind turbine designs have been substantially improved. The majority of MW-size turbines being installed today are capable of meeting the most severe grid code requirements, with advanced features including fault-ride-through capability. This enables them to assist in keeping the power system stable when disruptions occur. Modern wind farms are moving towards becoming wind energy power plants that can be actively controlled.

CHAPTER 3
DOUBLY FED INDUCTION GENERATOR

3.1 INTRODUCTION

With increased penetration of wind power into electrical grids, DFIG wind turbines are largely deployed due to their variable speed feature and hence influencing system dynamics. This has created an interest in developing suitable models for DFIG to be integrated into power system studies. As, grid codes are being revised to ensure that wind turbines would contribute to the control of voltage and frequency and also to stay connected to the host network following a disturbance.

In response to the new grid code requirements, the 3rd order model can be achieved by neglecting the rate of change of stator flux linkage, given rotor voltage as control parameter. Additionally, in order to model back-to back PWM converters, it is assumed that the converters are ideal and the DC-link voltage between the converters is constant. Consequently, depending on the converter control, a controllable voltage (current) source can be implemented to represent the operation of the rotor-side of the converter in the model. However, in reality DC-link voltage does not keep constant but starts increasing during fault condition.

A switch-by-switch representation of the back-to-back PWM converters with their associated modulators for both rotor- and stator-side Converters has been discussed. Hysteresis control has been deployed. However, hysteresis controller has two main disadvantages: firstly, the switching frequency does not remain constant but varies along the AC current waveform and secondly due to the roughness and randomness of the operation, protection of the converter is difficult. The latter will be of more significance when assessing performance of the system under fault condition. In order to resolve the identified problems, a switch-by-switch model of voltage-fed, current controlled PWM converters, triangular carrier-based Sinusoidal PWM (SPWM) is applied to maintain the switching frequency constant. In order to achieve constant switching frequency, calculation of the required rotor voltage that must be supplied to the generator is adopted. Synchronous PI controller has been adopted in order to control current-regulated induction

machine. Power quality is actually an important aspect in integrating wind power plants to grids. This is even more relevant since grids are now dealing with a continuous increase of non-linear loads such as switching power supplies and large AC drives directly connected to the network

Internal Model Control which is actually based on the concept of synchronous PI controllers. This method determines control parameters of the rotor-side converter of a DFIG, assuming ideal operation of back-to-back PWM converter. The approach may not be accurate enough due to the neglect of leakage factor. The same approach has been used by, while acknowledging leakage factor of induction machine, with DFIG controlled from the rotor-side. The same approach has been used, where dynamics of the PWM converters is taken into account along with the control of the DFIG from both stator- and rotor-side converters.

Wind turbines use a doubly-fed induction generator (DFIG) consisting of a wound rotor induction generator and an AC/DC/AC IGBT-based PWM converter. The stator winding is connected directly to the 50 Hz grid while the rotor is fed at variable frequency through the AC/DC/AC converter as shown in Fig. 3.1. The DFIG technology allows extracting maximum energy from the wind for low wind speeds by optimizing the turbine speed, while minimizing mechanical stresses on the turbine during gusts of wind. The optimum turbine speed producing maximum mechanical energy for a given wind speed is proportional to the wind speed. Another advantage of the DFIG technology is the ability for power electronic converters to generate or absorb reactive power.

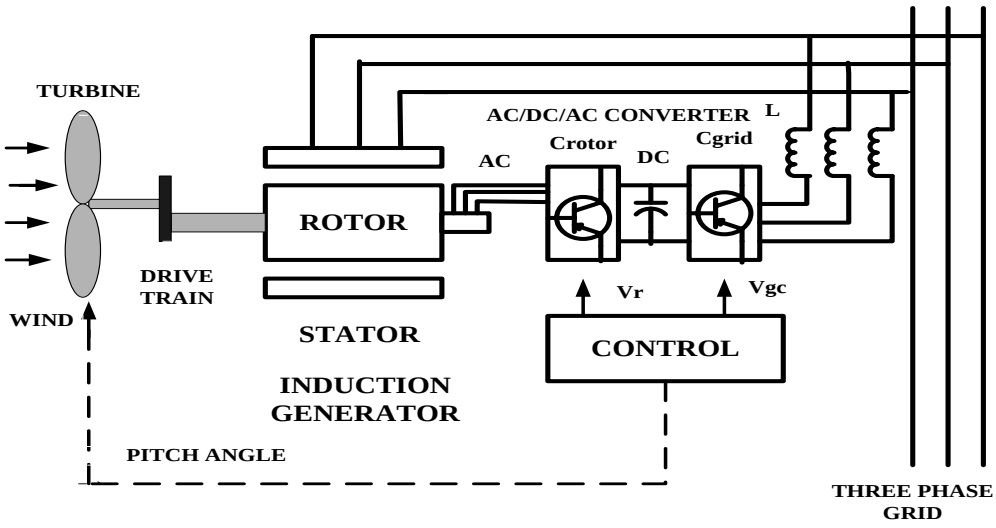

Fig 3.1 Basic Diagram of Doubly fed Induction Generator with converters

Where V_r is the rotor voltage and V_{gc} is grid side voltage. The AC/DC/AC converter is basically a PWM converter which uses sinusoidal PWM technique to reduce the harmonics present in the wind turbine driven DFIG system. Here C_{rotor} is rotor side converter and C_{grid} is grid side converter. To control the speed of wind turbine gear boxes or electronic control can be used.

3.2 OPERATING PRINCIPLE OF DFIG

The stator is directly connected to the AC mains, while the wound rotor is fed from the power converter via slip rings to allow DFIG to operate at a variety of speeds in response to changing wind speed. Fig. 3.2 shows the power flow diagram for DFIG. Indeed, the basic concept is to interpose a frequency converter between the variable frequency induction generator and fixed frequency grid. The DC capacitor linking stator-side and rotor-side converters allows the storage of power from induction generator for further generation. To achieve full control of grid current, the DC-link voltage must be boosted to a level higher than the amplitude of grid line-to-line voltage.

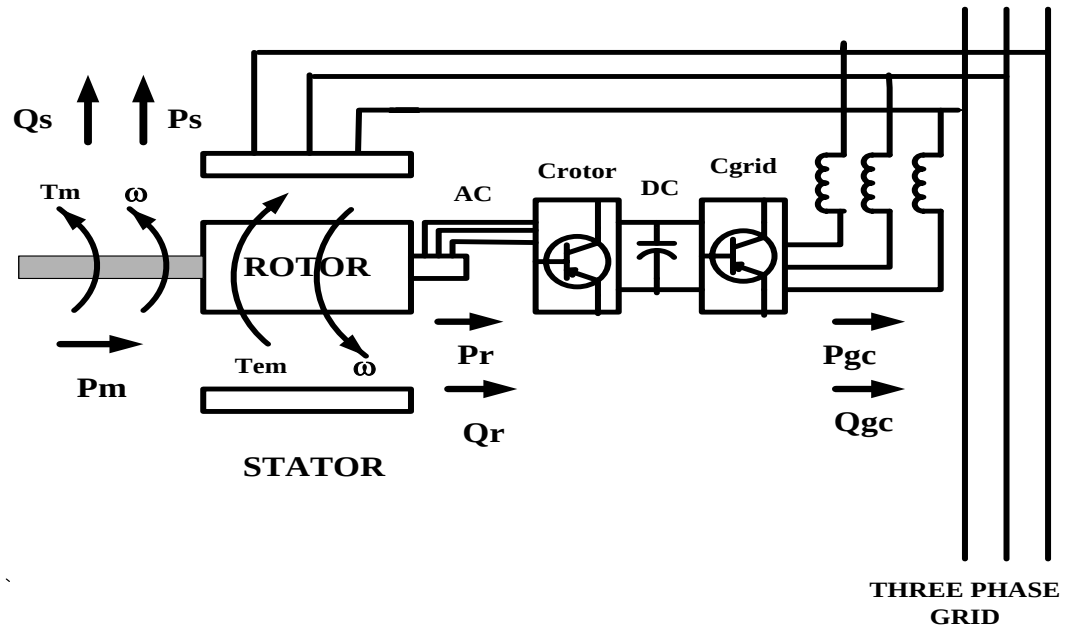

Fig. 3.2 Power flow diagram of DFIG

The slip power can flow in both directions, i.e. to the rotor from the supply and from supply to the rotor and hence the speed of the machine can be controlled from either rotor- or stator-side converter in both super and sub-synchronous speed ranges. As a result, the machine can be controlled as a generator or a motor in both super and sub-synchronous

operating modes realizing four operating modes. Below the synchronous speed in the motoring mode and above the synchronous speed in the generating mode, rotor-side converter operates as a rectifier and stator-side converter as an inverter, where slip power is returned to the stator. Below the synchronous speed in the generating mode and above the synchronous speed in the motoring mode, rotor-side converter operates as an inverter and stator side converter as a rectifier, where slip power is supplied to the rotor. At the synchronous speed, slip power is taken from supply to excite the rotor windings and in this case machine behaves as a synchronous machine.

The mechanical power and the stator electric power output are computed as follows:

$$P_r = T_m \omega_r \quad \text{.....(3.1)}$$

$$P_s = T_{em} \omega_s \quad \text{.....(3.2)}$$

For a loss less generator the mechanical equation is:

$$J \frac{d\omega_r}{dt} = T_m - T_{em} \quad \text{.....(3.3)}$$

In steady-state at fixed speed for a loss less generator

$$T_m = T_{em} \quad \text{.....(3.4)}$$

$$P_m = P_s + P_r \quad \text{.....(3.5)}$$

And it follows that:

$$P_r = P_m - P_s = T_m \omega_r - T_{em} \omega_s = -sP_s \quad \text{.....(3.6)}$$

Where, $s = \dfrac{(\omega_s - \omega_r)}{\omega_r}$, is defined as the slip of the generator

Generally the absolute value of slip is much lower than one and, consequently, Pr is only a fraction of Ps. Since Tm is positive for power generation and since ω_s is positive and constant for a constant frequency grid voltage, the sign of Pr is a function of the slip sign. Pr is positive for negative slip (speed greater than synchronous speed) and it is

negative for positive slip (speed lower than synchronous speed). For super-synchronous speed operation, Pr is transmitted to DC bus capacitor and tends to raise the DC voltage. For sub-synchronous speed operation, Pr is taken out of DC bus capacitor and tends to decrease the DC voltage. Cgrid is used to generate or absorb the power Pgc in order to keep the DC voltage constant. In steady-state for a lossless AC/DC/AC converter Pgc is equal to Pr and the speed of the wind turbine is determined by the power Pr absorbed or generated by Crotor. The phase-sequence of the AC voltage generated by Crotor is positive for sub-synchronous speed and negative for super-synchronous speed. The frequency of this voltage is equal to the product of the grid frequency and the absolute value of the slip. Crotor and Cgrid have the capability for generating or absorbing reactive power and could be used to control the reactive power or the voltage at the grid terminals.

3.3 DYNAMIC MODEL OF INDUCTION MACHINE

The Asynchronous Machine block operates in either generator or motor mode. The mode of operation is dictated by the sign of the mechanical torque:

- When Tm is positive, the machine acts as a motor.
- When Tm is negative, the machine acts as a generator.

The electrical part of the machine is represented by a fourth-order state-space model and the mechanical part by a second-order system. All electrical variables and parameters are referred to the stator. This is indicated by the prime signs in the machine equations given below. All stator and rotor quantities are in the arbitrary two-axis reference frame (dq frame) as shown in Fig. 3.3(a) and Fig. 3.3(b).

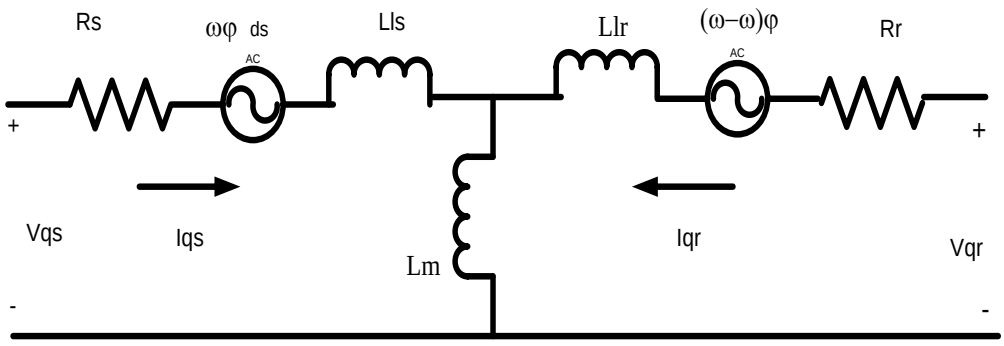

Fig.3.3(a)

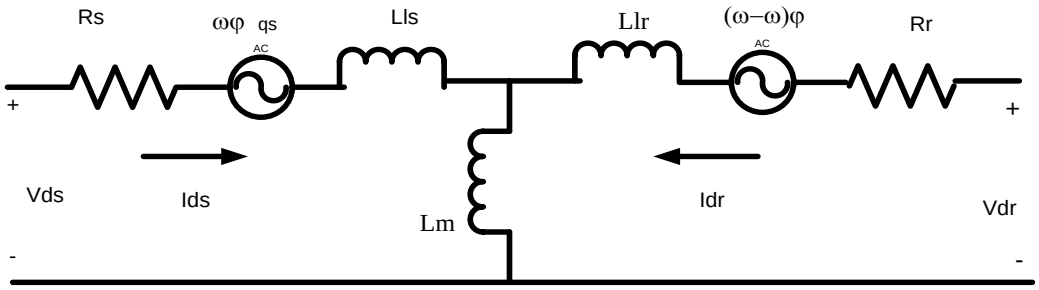

Fig.3.3 (b)

Equivalent Representation of d-q model of induction machine

To obtain the dynamic model, stator and rotor voltage equations, power and torque equations, stator and rotor flux linkage equations are needed. These equations are summarized as -

Stator Voltage Equations

$$V_{qs} = r_s i_{qs} + p\varphi_{qs} + \omega\varphi_{ds} \quad \text{.....(3.7)}$$

$$V_{ds} = r_s i_{ds} + p\varphi_{ds} - \omega\varphi_{qs} \quad \text{.....(3.8)}$$

Rotor Voltage Equations

$$V_{qr} = r_r i_{qr} + p\varphi_{qr} + (\omega - \omega_r)\varphi_{dr} \quad \text{..... (3.9)}$$

$$V_{dr} = r_r i_{dr} + p\varphi_{dr} - (\omega - \omega_r)\varphi_{qr} \quad \text{..... (3.10)}$$

Power Equations

$$P_s = \frac{3}{2}(V_{ds} i_{ds} + V_{qs} i_{qs}) \quad \text{.....(3.11)}$$

$$Q_s = \frac{3}{2}(V_{qs} i_{qs} - V_{ds} i_{ds}) \quad \text{.....(3.12)}$$

Torque Equation

$$T_e = 1.5p(\varphi_{ds} i_{qs} - \varphi_{qs} i_{ds}) \quad \text{.....(3.13a)}$$

$$\frac{d\theta_r}{dt} = k\left(\frac{1}{2H}\right) T_e - T_m - \omega_r \quad \text{.....(3.13b)}$$

Stator Flux Equations

$$\varphi_{qs} = (L_{ls} + L_m) i_{qs} + L_m i_{qr} \quad \text{.....(3.14)}$$

$$\varphi_{ds} = (L_{ls} + L_m) i_{ds} + L_m i_{dr} \quad \text{..... (3.15)}$$

Rotor Flux Equations

$$\varphi_{qr} = (L_{lr} + L_m) i_{qr} + L_m i_{qs} \quad \text{..... (3.16)}$$

$$\varphi_{dr} = (L_{lr} + L_m) i_{dr} + L_m i_{ds} \quad \text{.....(3.17)}$$

3.4 MODEL OF PWM CONVERTER AND CONTROL SCHEME

Mathematical modeling of converter system is realized by using various types of models, which can be broadly divided into two groups: mathematical functional models and Mathematical physical models (either equation-oriented or graphic-oriented, where graphic-oriented approach is actually based on the same differential equations). Functional model describes the relationship between the input and output signal of the system in form of mathematical function(s) and hence constituting elements of the system are not modeled separately.

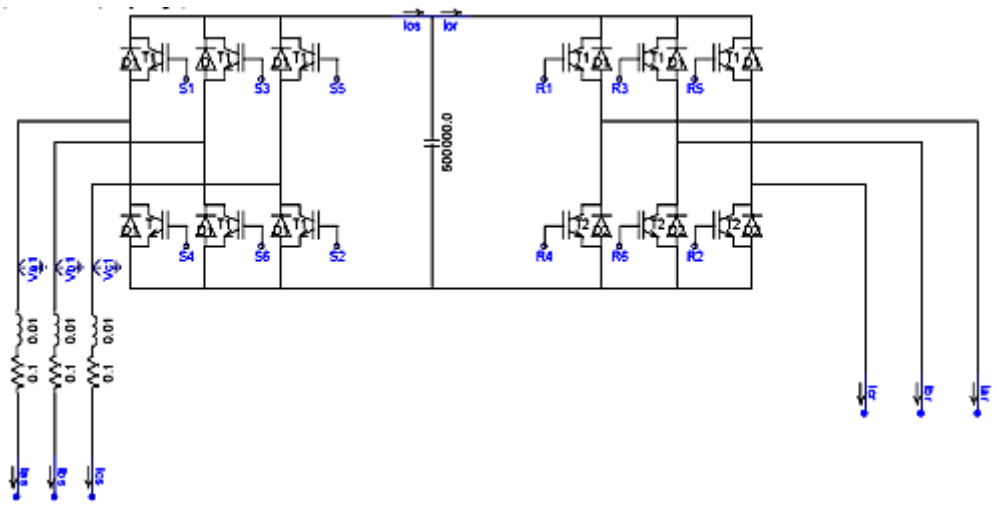

Fig.3.4 Back-to-back PWM converter structure

Physical model constitutes elements of the system separately and also considers interrelationship among different elements within the system, where type and structure of the model is normally dictated by the particular requirements of the analysis, e.g. steady-state, fault studies, etc. Graphic-oriented switch-by-switch representation of the back-to-back PWM converters with their modulators for both rotor-side and stator-side converters, are represented in Fig. 3.5 as a resistive switch.

A voltage-source, current controlled PWM converter is used. The main task of the control in the Current Controlled PWM converter is to force the current to follow their reference signals. By comparing desired and actual values of the phase currents, the Current Controlled generates the switching states for converter which decreases the current errors. There are various ways to obtain the switching signals for the inverter switches in order to control the inverter output current. The simplest is hysteresis control, where the actual current is compared to the desired current in each phase leg of the converter output. Sinusoidal Pulse Width Modulation (SPWM) method is adopted, which is based on a triangular carrier signal. By comparison of the common carrier signal with three reference sinusoidal signals the switching instants of the IGBTs are obtained. In order to maintain the switching frequency within the switch-mode converter constant, it is a best to calculate the required rotor voltages that the converter must supply to the machine, making the rotor currents equal to their reference values. The control of generator and converter can be explained as following-

3.4.1 ROTOR-SIDE CONTROL

Aligning the d-axis of reference frame to be along the stator flux linkage (stator flux oriented control) will result in:

$$\varphi_{qs}^{e} = 0 \quad \text{..... (3.18)}$$

And hence from Eq. (3.14):

$$i_{qs}^{e} = -\frac{L_m}{L_{ls} + L_m} i_{qr}^{e} \quad \text{.....(3.19)}$$

Substituting for i_{qs}^{e} into Eq. (3.13) will result in:

$$T_e = -\frac{3}{2}\frac{P}{2}\frac{L_m}{L_{ls}+L_m}\varphi_{ds}^e i_{qr}^e \quad \text{.....(3.20)}$$

For φ_{ds}^e to remain unchanged at zero, $p\varphi_{ds}$ must be zero. Substituting for $p\varphi_{ds}$ using equation (3.7) and (3.8) will result in $V_{ds}^e = r_s i_{ds}^e$. Neglecting stator resistance will lead to $V_{ds}^e = 0$. Substituting for $V_{ds}^e = 0$, eqs. (3.11) and (3.12) will be simplified as follows:

$$P_s^e = \frac{3}{2}(V_{qs}^e i_{qs}^e) \quad \text{.....(3.21)}$$

$$Q_s^e = \frac{3}{2}(V_{qs}^e i_{ds}^e) \quad \text{.....(3.22)}$$

Therefore, the above equations show that active and reactive powers of the stator can be controlled independently.

3.4.2 DECOUPLING CONTROL SCHEME

Using stator flux oriented approach with current controlled PWM inverter requires decoupling scheme. In fact, the system is coupled because the inductance matrix is not diagonal. It means that any changes on voltage component in d or q axes results in changes in both current components. In order to combat this problem, equations will be re-developed in order to compensate for these cross coupling between d and q axes.

Leakage factor of the induction machine can be defined as:

$$\sigma = 1 - \frac{L_m^2}{(L_{ls}+L_m)(L_{lr}+L_m)} \quad \text{..... (3.23)}$$

Substituting for i_{ds}^e from Eq. (3.15) into Eq. (3.17) for λ_{dr}^e and from Eq. (3.19) into Eq.(3.16)

$$\varphi_{dr}^e = \sigma(L_{lr}+L_m)i_{dr}^e + \frac{L_m}{L_{ls}+L_m}\varphi_{ds}^e \quad \text{..... (3.24)}$$

$$\varphi_{qr}^e = \sigma(L_{lr}+L_m)i_{qr}^e \quad \text{..... (3.25)}$$

Substituting above equations into Eq. (3.9) and (3.10) for V_{qr}^{e} and V_{dr}^{e}

$$V_{dr}^{e} = V_{dr}^{'e} + V_{dr,comp}^{e} \quad \text{(3.26)}$$

$$V_{qr}^{e} = V_{qr}^{'e} + V_{qr,comp}^{e} \quad \text{(3.27)}$$

Where,

$$V_{dr}^{'e} = r_r i_{dr}^{e} + \sigma(L_{lr} + L_m) p i_{dr}^{e} \quad \text{(3.28)}$$

$$V_{qr}^{'e} = r_r i_{qr}^{e} + \sigma(L_{lr} + L_m) p i_{qr}^{e} \quad \text{(3.29)}$$

$$V_{dr,comp}^{e} = \frac{L_m}{L_{ls} + L_m} p i_{ds}^{e} - (\omega_e - \omega_r)\sigma(L_{lr} + L_m) i_{qr}^{e} \quad \text{(3.30)}$$

$$V_{qr,comp}^{e} = (\omega_e - \omega_r)\frac{L_m}{L_{ls} + L_m} \varphi_{ds}^{e} + (\omega_e - \omega_r)\sigma(L_{lr} + L_m) i_{dr}^{e} \quad \text{(3.31)}$$

Adding these compensating terms to the corresponding uncompensated voltage terms makes it possible to achieve decoupled performance of the stator flux-oriented control of the rotor-side converter.

3.4.3 STATOR-SIDE CONTROL

The main objective of stator-side converter is to maintain the DC-link voltage constant regardless of the magnitude and direction of the slip power. A current-regulated PWM scheme is used, where q and d axes currents are used to regulate DC-link voltage and reactive power, respectively. Based on Fig.3.2 and taking into account the inductance and resistance of the input filter, voltage equations across the inductor can be written as follows:

$$\begin{bmatrix} V_{as} \\ V_{bs} \\ V_{cs} \end{bmatrix} = R \begin{bmatrix} i_{as} \\ i_{bs} \\ i_{cs} \end{bmatrix} + Lp \begin{bmatrix} i_{as} \\ i_{bs} \\ i_{cs} \end{bmatrix} + \begin{bmatrix} V_{a1} \\ V_{b1} \\ V_{c1} \end{bmatrix} \quad \text{(3.32)}$$

Applying phase and rotation transformations to the above equation results in:

$$V_{ds}^{e} = Ri_{ds}^{e} + Lpi_{ds}^{e} - \omega_e Li_{qs}^{e} + V_{d1}^{e} \quad (3.33)$$

$$V_{qs}^{e} = Ri_{qs}^{e} + Lpi_{qs}^{e} - \omega_e Li_{ds}^{e} + V_{q1}^{e} \quad (3.34)$$

Therefore, reference values for front-end converter can be written as:

$$V_{d1}^{ref,e} = -Ri_{ds}^{e} - Lpi_{ds}^{e} + (\omega_e Li_{qs}^{e}) \quad (3.35)$$

$$V_{q1}^{ref,e} = -Ri_{qs}^{e} - Lpi_{qs}^{e} + (\omega_e Li_{ds}^{e} - V_{qs}^{e}) \quad (3.36)$$

Where, the term in bracket represents the decoupling terms. Neglecting harmonics, the capacitor leakages and losses in the inductor resistance and converter itself.

$$Ei_{os} = \frac{3}{2} V_{qs}^{e} i_{qs}^{e} \quad (3.37)$$

$$V_{qs}^{e} = \frac{M_1}{2\sqrt{2}} E \quad (3.38)$$

$$i_{os} = \frac{3}{4\sqrt{2}} M_1 i_{qs}^{e} \quad (3.39)$$

$$CpE = i_{os} - i_{or} \quad (3.40)$$

Assuming rotor-side converter DC-link current as disturbance and combining eqs. (3.39) and (3.40)

$$E = \frac{3}{4\sqrt{2}} M_1 i_{os} \quad (3.41)$$

3.5 CONTROLLER DESIGN

The controller design is explained through following steps-

3.5.1 BASICS OF INTERNAL MODEL CONTROLLER

The idea behind IMC is to augment the error between system, G(S), and the model of the system, $\hat{G}(s)$, by a transfer function C(S). For a first-order system the controller is an ordinary PI controller which can be represented as follows:

$$F(s) = k_p + \frac{k_i}{s} = \frac{\alpha}{s}\hat{G}^{-1}(s) \quad \text{..... (3.42)}$$

Where, $\hat{G}(s)$ is the transfer function of the system.

3.5.2 SUPPLY-SIDE CONVERTER

In simplified design the small time constants such as power converter dead time, feedback filter and digital signal processing delay are neglected. Thus, only the dynamics of supply-side filter is taken into account. Fig.3.5 shows the current-control loop of stator-side converter. Based on eqs.(3.35) and (3.36) and considering compensation terms as disturbance, the plant for the **current control loop** is given by:

$$\hat{G}(s) = \frac{i_{ds}^{e}(s)}{(R+Ls)i_{ds}^{e}(s)} = \frac{i_{qs}^{e}(s)}{(R+Ls)i_{qs}^{e}(s)} = \frac{1}{R+Ls} \quad \text{..... (3.43)}$$

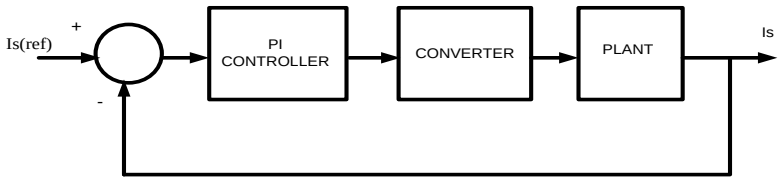

Fig.3.5 Current-control loop of stator-side converter

Given converter model as:

$$k_{cs} = \frac{M_1 E}{2V_{tri}} \quad \text{..... (3.44)}$$

And substituting for Eq. (3.40)

$$k_p = \frac{\alpha_{cs} L}{k_{cs}} \quad \text{..... (3.45)}$$

$$k_i = \frac{\alpha_{cs} R}{k_{cs}} \quad \text{.....(3.46)}$$

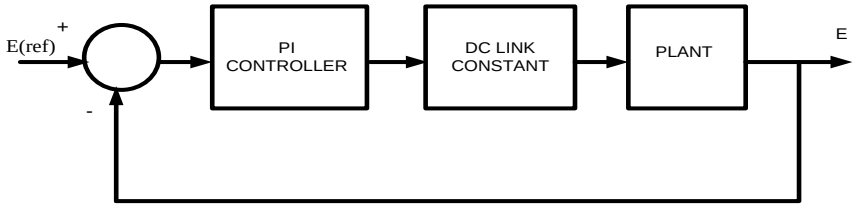

Fig.3.6 DC-link voltage-control loop

Based on fig.3.6 and given **DC-Link transfer characteristic**s from Eq. (3.40) and plant transfer function as:

$$E = \frac{3M_1}{4\sqrt{2}} i_{os} \quad \text{(3.47)}$$

$$\hat{G}(s) = \frac{1}{Cs} \quad \text{(3.48)}$$

And substituting for Eq.(3.41) leads to

$$k_p = \frac{4\sqrt{2}\alpha_E C}{3M_1} \quad \text{(3.49)}$$

There will be a remaining error when the induction machine is loaded and active power flows between DC-link and the machine. The remaining error can be eliminated by adding an integrator to the DC-link voltage controller. The following is often adopted for the selection of the controller integration time:

$$T_i = \frac{10}{\alpha_E} \quad \text{(3.50)}$$

Where, $T_i = \frac{k_P}{k_i}$ (3.51)

3.5.3 ROTOR-SIDE CONVERTER

As mentioned previously, in order to keep the switching frequency constant, it is necessary to calculate the required rotor voltages. The iqr and idr errors are processed by the **PI controller** to give Vqr and Vdr, respectively. Using Eq. (3.28) and (3.29), the plant can be represented by transfer functions below:

$$i_{dr}^{e}(s) = \frac{1}{r_r + s\sigma(L_{lr} + L_m)} V_{dr}^{'e}(s) \quad \text{(3.52)}$$

$$i_{qr}^{e}(s) = \frac{1}{r_r + s\sigma(L_{lr} + L_m)} V_{qr}^{'e}(s) \quad \text{(3.53)}$$

Therefore, the transfer function of the Plant is given by:

$$\hat{G}(s) = \frac{1}{r_r + s\sigma(L_{lr} + L_m)} \quad \text{.....(3.54)}$$

Incorporating dynamics of PWM converter makes the block diagram as shown in Fig.3.7. Where converter can be represented as:

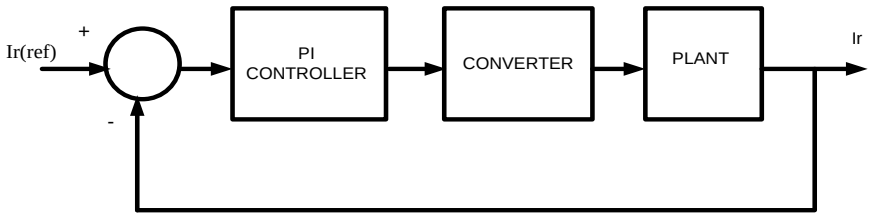

Fig.3.7 Designing current-control loop for constant switching frequency

$$k_{cr} = \frac{M_2 E}{2V_{tri}} \quad \text{..... (3.55)}$$

This will determine control parameters as follows:

$$k_p = \frac{\alpha_{cr}\sigma(L_{lr} + L_m)}{k_{cr}} \quad \text{..... (3.56)}$$

$$k_i = \frac{\alpha_{cr} r_r}{k_{cr}} \quad \text{..... (3.57)}$$

Assuming single-mass representation of the mechanical drive train and using Fig.3.8, plant transfer function for **speed controller** is given by:

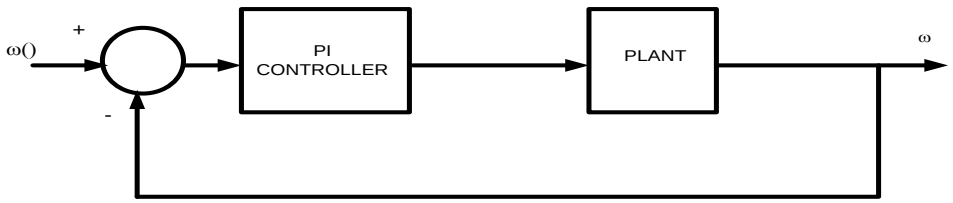

Fig.3.8 Speed control loop of DFIG

$$\hat{G}(s) = \frac{1}{JS + D} \quad \text{..... (3.58)}$$

$$k_{p\omega} = \frac{\alpha_\omega JP}{2} \quad \text{..... (3.59)}$$

$$k_{i\omega} = \alpha_\omega D \quad \text{..... (3.60)}$$

CHAPTER 4
HVDC TRANSMISSION SYSTEM

4.1 INTRODUCTION

The industrial growth of nation requires increased consumption of energy, particularly electrical energy. This has led to the increase in the generation and transmission facilities to meet the energy demands. In modern countries, till early seventies, the demand doubles after ten years. In developing countries demand doubles in every seven years which requires considerable investment in power sector.

Remote generation and system interconnection lead to search for efficient power transmission at increasing power levels. The increase in voltage levels is not always feasible. The problems with long distance AC transmission had led to development of the High Voltage Direct Current (HVDC) Transmission. However, as generation and utilization of power remain at alternating current, HVDC transmission requires conversion at two ends from AC to DC at sending end and DC to AC at receiving end. The HVDC technology still undergoing many changes due to continuing innovation directed at improving reliability and reducing costs of converter stations. The HVDC systems are quiet reliable as converter control allows flexibility in system operation, full realization of the potential benefits. HVDC transmission requires detailed study during the planning and design stage. This necessitates proper modeling and analysis of HVDC systems. The successful use of thyristors for power control in industrial devices encouraged its adoption in HVDC converters by development of high power semiconductor devices.

The HVDC technology is a high power electronics technology used in electric power systems. It is an efficient and flexible method to transmit large amounts of electric power over long distances by overhead transmission lines or underground/submarine cables. It can also be used to interconnect asynchronous power systems. Nowadays, the HVDC is being widely used all around the world. Until recently HVDC based on thyristors, which is called traditional HVDC, has been used for conversion from AC to DC and vice versa. Recently a new type of HVDC has become available. It makes use of the more advanced semiconductor technology instead of thyristors for power conversion between AC and DC. The semiconductors used are insulated gate bipolar transistors

(IGBTs), and the converters are voltage source converters (VSCs) which operate with high switching frequencies (1-2 kHz) utilizing pulse width modulation (PWM).

Owning to IGBT valves, VSC–HVDC systems allows independent and total control of active and reactive power at each end of the line and power transmission can be controlled with high flexibility. VSC–HVDC can address not only conventional network issues such as bulk power transmission, asynchronous network interconnections, back–to–back AC system linking and voltage/stability support, but also niche markets such as the integration of large scale renewable energy sources with the grid.

4.2 PRINCIPLE OPERATION OF HVDC TRANSMISSION SYSTEM

A high-voltage, direct current (HVDC) electric power transmission system uses direct current for the bulk transmission of electrical power, in contrast with the more common alternating current systems. For long-distance distribution, HVDC systems are less expensive and suffer lower electrical losses. Also to provide an asynchronous link between two ac systems, it is necessary to have a dc system in place. The dc system basically has two converter stations one at each end, connected by dc transmission line as shown in Fig. 4.1. The generated ac power is fed to the dc transmission line through converter station that that comprises transformers and thyristor valves.

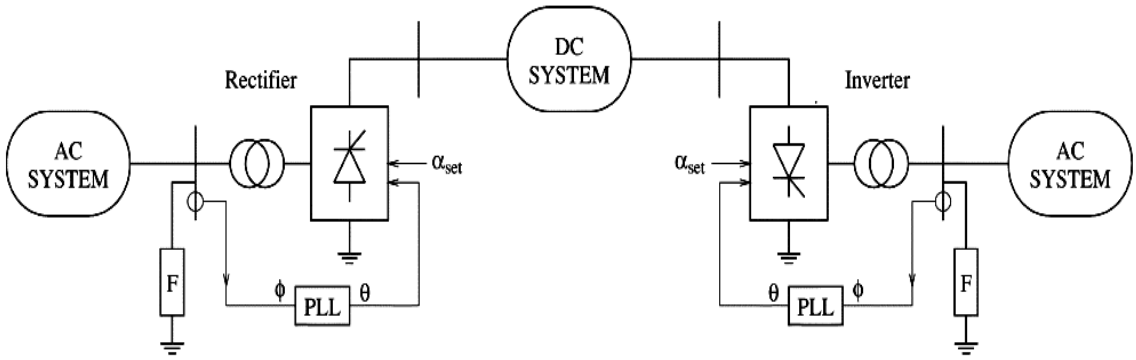

Fig 4.1 HVDC Transmission System Model

The dc output voltage magnitude is controlled by varying the firing angle of thyristor valves in the converter. In rectifier the firing angle is between 0^0 to 90^0 while in inverter is in between 90^0 to 180^0.

4.3 CONFIGURATIONS OF HVDC SYSTEMS

HVDC converter bridges together with lines or cables can be arranged in a number of Configurations. These configurations are-

- **Monopole System**
- **Bipolar System**
- **Homopolar System**

In a common configuration, called **monopole** as shown in Fig. 4.2., one of the terminals of the rectifier is connected to earth ground. The other terminal, at a potential high above, or below, ground, is connected to a transmission line. The earthed terminal may or may not be connected to the corresponding connection at the inverting station by means of a second conductor. If no metallic conductor is installed, current flows in the earth between the earth electrodes at the two stations. Therefore it is a type of single wire earth return. Since one terminal of the converters is connected to earth, the return conductor need not be insulated for the full transmission voltage which makes it less costly than the high-voltage conductor. Use of a metallic return conductor is decided based on economic, technical and environmental factors. Modern monopolar systems for pure overhead lines carry typically 1,500 MW. If underground or underwater cables are used the typical value is 600 MW.

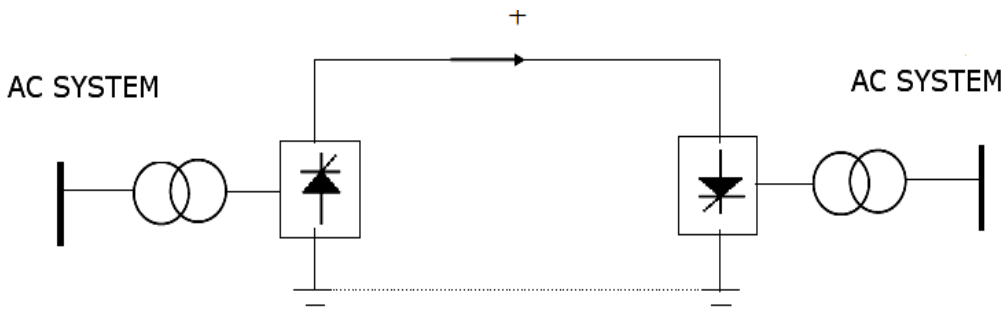

Fig.4.2 Monopolar System

Bipolar transmission as shown in Fig. 4.3 consist a pair of conductors is used, each at a high potential with respect to ground, in opposite polarity. Since these conductors must be insulated for the full voltage, transmission line cost is higher than a monopole with a return conductor. Under normal load, negligible earth-current flows, as in the case

of monopolar transmission with a metallic earth-return. This reduces earth return loss and environmental effects. When a fault develops in a line, with earth return electrodes installed at each end of the line, approximately half the rated power can continue to flow using the earth as a return path, operating in monopolar mode. A bipolar system may also be installed with a metallic earth return conductor. Bipolar systems may carry as much as 3,200 MW at voltages of +/-600 kV.

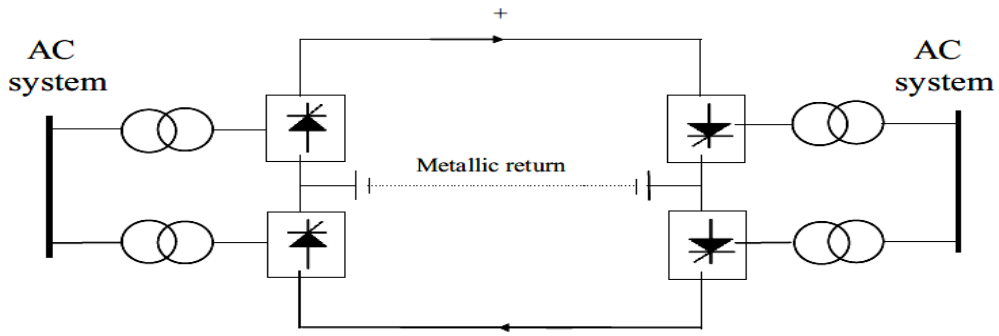

Fig.4.3 Bipolar System

Homopolar link has two or more conductors having same polarity (usually negative), and always operates with ground return. The homopolar link is shown in fig 4.4.The main advantage of homopolar link is that a negative polarity causes less radio interference due to corona.

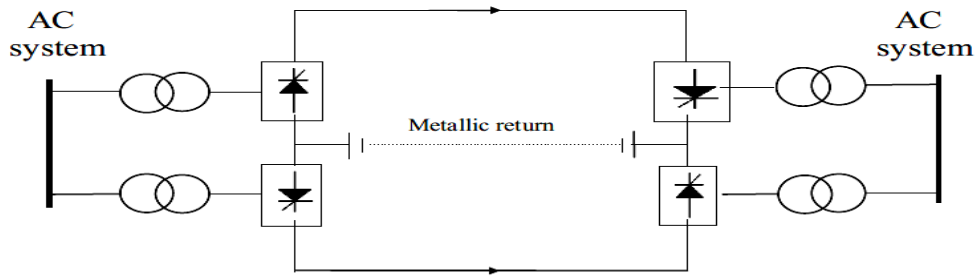

Fig.4.4 Homopolar System

4.4 MAIN COMPONENTS OF HVDC SYSTEM

In an HVDC system, AC is converted in DC by means of a combination of converter transformers and converter valves. The rectifier and inverter normally control the DC current flowing in the circuit and do this by adjusting its output DC voltage to give

a current flow. The main components for the HVDC system are shown in Fig. 4.5. The components are-

- **Converters**
- **Transformers**
- **DC capacitors**
- **Cables**
- **Filters**

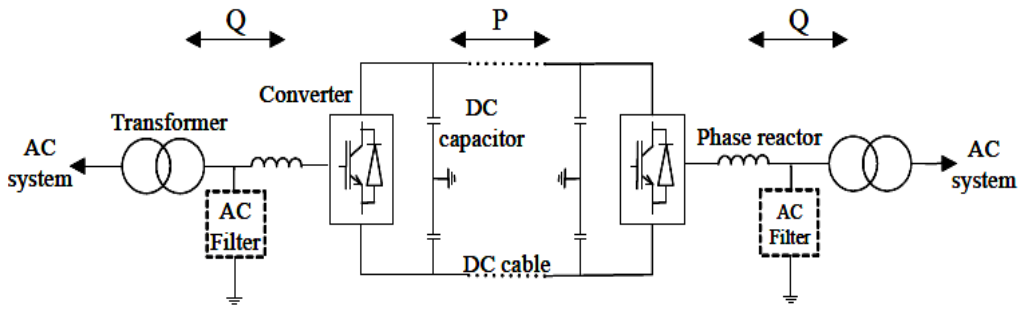

Fig.4.5 Main Components of HVDC System

Conversion from AC to DC (Rectifier Station) and conversion from DC to AC (Inverter Station) is performed by **converters**, and consists of valve groups and transformers with tap changers. A point-to-point transmission requires two converters. The role of converter and inverter stations can be reversed (resulting in power reversals) by suitable converter control. Converter unit usually consists of three phase Converter Bridge arranged in 6 pulse or 12 pulse. The converter fed from converter transformer connected in star/star or delta/star arrangement. Converter valves firing signals are generated in the converter control at the ground potential and are transmitted to each thyristor. The light signal received at the thyristor level is converted into electrical signal using gate drive amplifier with pulse transformers. The converter valves are protected using damper circuit and protective firing. Converter transformer can have different configurations (i) three phase two winding (ii)single phase, three winding. The converter side is connected in star or in delta connection. On the AC side, the transformer winding is connected in star connection with point grounded. The transformers are designed to withstand harmonic DC voltage stresses and increased eddy current losses due to harmonic currents.

Normally, the converters are connected to the AC system via **transformers**. The most important function of the transformers is to transform the voltage of the AC system

to a level suitable for the converter. For six-pulse converter, a conventional 3-phase or three single phase transformers is used. Converter transformers are specially designed power transformers differing in many respects from the usual power transformer. The valve side transformer windings are designed to withstand alternating voltage stress and direct voltage stress from Valve Bridge. The current flowing through the windings consists of high harmonic contents. Thus the losses due to eddy current are high. The noise due to magnatostriction is higher and may require specially designed tank. Converter transformers serve several functions.

- Voltage transformation between the AC supply and the HVDC system.
- Supply of AC voltages in two separate circuits with a relative phase shift of 30electrical degrees for reduction of low order harmonics, especially the 5th and 7^{th} harmonics.
- Act as a galvanic barrier between the AC and DC systems to prevent the DC potential to enter the AC system.
- Reactive impedance in the AC supply to reduce short circuit currents and to control the rate of rise of valve current.

DC capacitors are placed on the DC side and the main goal is to provide a low inductive path for the turned-off current and an energy buffer to control the power flow. If disturbances happen in the AC system the result will be variations in the DC voltage. The aim of there capacitors is to limit these variations. The proper sizing of these capacitors is essential in an HVDC system. Because of the switching frequency of the PWM converter, the current flowing to the DC side contains harmonics which will result in a ripple on the DC side voltage. The magnitude of ripples depends on the size of the DC capacitor and on the switching frequency.

Using DC **cables** for connecting the offshore wind farms to different systems offers several advantages such as better transmission efficiency for long distances and high powers, no magnetic losses, less weight then AC cables. The used cables have polymeric insulating material which provides them strength and flexibility, reasons that makes then suitable for severe installation conditions like submarine. The total capacitance of the DC link model is characterized by the converters and the cable DC bus capacitance. For modeling the DC cables, a π–model is used.

The currents and the voltages at the inverter and rectifier are not sinusoidal due to the commutation valve switching process. These non-sinusoidal current and voltage waveforms consist of the fundamental frequency AC component plus higher-order harmonics. Connecting a voltage source converter to the transmission system the voltage must be sinusoidal and this is accomplished by using reactors and AC **filters.** Voltage source converters based on PWM is controlling the ratio between the fundamental voltage frequency on the DC and AC side. One advantage of using voltage source converters is that no reactive power compensation is needed, therefore the number of filters will be reduced and the current harmonics on the AC side are related only to the PWM frequency.

4.5 MODELING OF HVDC SYSTEMS

The modeling of the HVDC components is realized in the dq synchronous reference frame since the control will be implemented in the same reference frame. Fig.4.6 shows a schematic representation of the HVDC VSC link that is going to be modeled. It consists of two three-phase sources, left and right side of the figure, which represent the equivalent electrical systems that are connected by the DC link. The DC Link is composed of two VSC converters connected by a DC cable. It is important to notice the inductances between the three-phase sources and the converters. These inductances are fundamental in order to allow active and reactive powers at both sides of the DC link to be controlled. The resistances that are in series with these inductances represent the power losses in the converters. Then the resistance and inductance in the DC cable represent its resistance and self inductance, respectively.

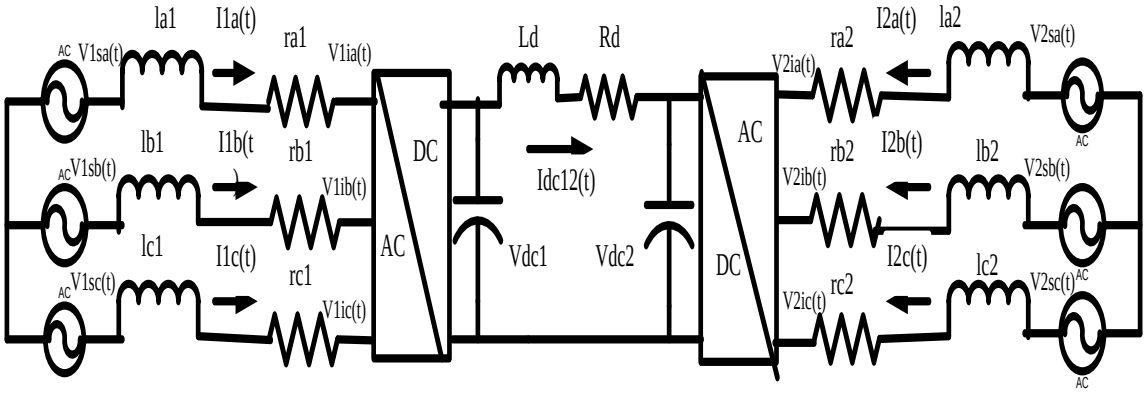

Fig.4.6 Voltage Source Converter based High Voltage Direct Current

Applying voltage Kirchhoff law to the left **AC side** yields:

$$\begin{bmatrix} v_{1sa} \\ v_{1sb} \\ v_{1sc} \end{bmatrix} - R_1 \begin{bmatrix} i_{1a} \\ i_{1b} \\ i_{1c} \end{bmatrix} - L_1 \frac{d}{dt} \begin{bmatrix} i_{1a} \\ i_{1b} \\ i_{1c} \end{bmatrix} - \begin{bmatrix} v_{1ia} \\ v_{1ib} \\ v_{1ic} \end{bmatrix} = \begin{bmatrix} 0 \\ 0 \\ 0 \end{bmatrix} \quad \text{.....(4.1)}$$

$$v_{1sa} = V_1 \sqrt{\frac{2}{3}} \sin(\omega t + \theta_1)$$

$$v_{1sb} = V_1 \sqrt{\frac{2}{3}} \sin(\omega t + \theta_1 - \frac{2\Pi}{3})$$

$$v_{1sc} = V_1 \sqrt{\frac{2}{3}} \sin(\omega t + \theta_1 + \frac{2\Pi}{3}) \quad \text{.....(4.2)}$$

$$v_{1ia} = kM_1 v_{1dc} \sin(\omega t + \theta_1 + \delta_1)$$

$$v_{1ib} = kM_1 v_{1dc} \sin(\omega t + \theta_1 + \delta_1 - \frac{2\Pi}{3})$$

$$v_{1ic} = kM_1 v_{1dc} \sin(\omega t + \theta_1 + \delta_1 + \frac{2\Pi}{3}) \quad \text{.....(4.3)}$$

The resistance and inductance matrices are defined as $R_1 = diag(r_{a1}, r_{b1}, r_{c1})$ and $L_1 = diag(l_{a1}, l_{b1}, l_{c1})$ respectively. The equations corresponding to the right-hand side device are obtained by just exchanging the subscript "1" by "2". Then the equations can be written in a compact form as follows:

$$v_{1s}^{abc} - R_1 i_1^{abc} - L_1 \frac{di_1^{abc}}{dt} - v_{1i}^{abc} = 0 \quad \text{.....(4.4)}$$

$$v_{2s}^{abc} - R_2 i_2^{abc} - L_2 \frac{di_2^{abc}}{dt} - v_{2i}^{abc} = 0 \quad \text{.....(4.5)}$$

The following Park transformation:

$$P = \frac{2}{3} \begin{bmatrix} \cos(\omega t) & \cos(\omega t - \frac{2\Pi}{3}) & \cos(\omega t + \frac{2\Pi}{3}) \\ -\sin(\omega t) & -\sin(\omega t - \frac{2\Pi}{3}) & -\sin(\omega t + \frac{2\Pi}{3}) \\ \frac{1}{2} & \frac{1}{2} & \frac{1}{2} \end{bmatrix} \quad \text{.....(4.6)}$$

and its inverse P^{-1}, can be applied in abc coordinates, X^{abc}, to transform the system into the synchronous rotating reference frame D -Q, whose coordinates are $x = x^{dq0}$. Then the relation between the two coordinate systems is $x^{dq0} = Px^{abc}$ and $x^{abc} = P^{-1}x$. Applying this to (4.4) and (4.5) a D -Q model is obtained as follows:

$$P^{-1}v_{1s} - R_1P^{-1}i_1 - L_1\frac{d(P^{-1}i_1)}{dt} - P^{-1}v_{1i} = 0 \quad \text{.....(4.7)}$$

$$P^{-1}v_{2s} - R_2P^{-1}i_2 - L_2\frac{d(P^{-1}i_2)}{dt} - P^{-1}v_{2i} = 0 \quad \text{.....(4.8)}$$

Multiplying by P:

$$v_{1s} - R_1i_1 - L_1\frac{d(P^{-1}i_1)}{dt} - v_{1i} = 0 \quad \text{.....(4.9)}$$

$$v_{2s} - R_2i_2 - L_2\frac{d(P^{-1}i_2)}{dt} - v_{2i} = 0 \quad \text{.....(4.10)}$$

Where, the dq0 currents for both devices are defined as follows:

$$i_1 = \begin{bmatrix} i_{1d} \\ i_{1q} \\ i_{10} \end{bmatrix} \quad i_2 = \begin{bmatrix} i_{2d} \\ i_{2q} \\ i_{20} \end{bmatrix} \quad \text{.....(4.11)}$$

On the other hand, the voltages in dq0 reference frame are:

$$v_{1s} = Pv_{1s}^{abc} = \begin{bmatrix} v_{1sd} \\ v_{1sq} \\ v_{1s0} \end{bmatrix} = \begin{bmatrix} v_1\sqrt{\frac{2}{3}}\sin(\theta_1) \\ -v_1\sqrt{\frac{2}{3}}\cos(\theta_1) \\ 0 \end{bmatrix} \quad \text{.....(4.12)}$$

$$v_{1i} = Pv_{1i}^{abc} = \begin{bmatrix} v_{1id} \\ v_{1iq} \\ v_{1i0} \end{bmatrix} = \begin{bmatrix} kM_1v_{dc1}\sin(\theta_1 + \delta_1) \\ -kM_1v_{dc1}\cos(\theta_1 + \delta_1) \\ 0 \end{bmatrix} \quad \text{.....(4.13)}$$

$$v_{2s} = Pv_{2s}^{abc} = \begin{bmatrix} v_{2sd} \\ v_{2sq} \\ v_{2s0} \end{bmatrix} = \begin{bmatrix} v_1\sqrt{\frac{2}{3}}\sin(\theta_2) \\ -v_1\sqrt{\frac{2}{3}}\cos(\theta_2) \\ 0 \end{bmatrix} \quad \text{.....(4.14)}$$

$$v_{2i} = Pv_{2i}^{abc} = \begin{bmatrix} v_{2id} \\ v_{2iq} \\ v_{2i0} \end{bmatrix} = \begin{bmatrix} kM_2 v_{dc2}\sin(\theta_2 + \delta_2) \\ -kM_2 v_{dc2}\cos(\theta_2 + \delta_2) \\ 0 \end{bmatrix} \quad \text{.....(4.15)}$$

Considering that the resistances and reactances are the same in each phase they can be written as $r_1 = r_{al} = r_{bl} = r_{cl}$ and $1_1 = l_{al} = l_{bl} = l_{c1}$, and similarly for the right-hand side device. Then, denoting $L_1=l_1 I$ and $R_1=r_1 I$, with I the identity matrix, yields:

$$L_1 P\frac{d(P^{-1}i_1)}{dt} = l_1\frac{d}{dt}\begin{bmatrix} i_{1d} \\ i_{1q} \\ 0 \end{bmatrix} + l_1\begin{bmatrix} -i_{1q}\omega \\ i_{1d}\omega \\ 0 \end{bmatrix} \quad \text{.....(4.16)}$$

And, same for the other end converter.

Applying voltage Kirchhoff law to the **DC-Link**:

$$v_{dc1} - R_d i_{dc12} - L_d\frac{di_{dc12}}{dt} + v_{dc1} = 0 \quad \text{.....(4.17)}$$

$$i_{dc1} - C_1\frac{dv_{dc1}}{dt} - i_{dc12} = 0 \quad \text{.....(4.18)}$$

The dynamic model for the DC system is obtained as follows:

$$i_{dc2} - C_2\frac{dv_{dc2}}{dt} - i_{dc12} = 0 \quad \text{.....(4.19)}$$

The **coupling** between the **AC and DC sides** can be based in the power conservation principle. For the left AC side, the power at IGBT's AC terminals is:

$$p_{1iac}^{abc} = v_{1i}^{abc}(i_1^{abc})^T \quad \text{.....(4.20)}$$

$$p_{1dc} = i_{dc1} v_{dc1} \quad \text{..... (4.21)}$$

It is supposed that the losses in the converters are represented by the resistances r_1 and r_2, included in the circuit but not in the converters. Then, the converters are considered lossless, which means that the powers on the AC sides equal the power in the DC sides.

$$p_{1iac}^{abc} = p_{1dc} \quad \text{.....(4.22)}$$

In the dq0 reference frame equation (4.20) can be written as:

$$p_{1iac}^{abc} = v_{1i}^{abc} (i_1^{abc})^T = p_{1iac} = (P^{-1} v_{1i})(P^{-1} i_1)^T$$
$$= \frac{3}{2}[v_{1id} i_{1d} + v_{1iq} i_{1q} + 2 v_{1i0} i_{10}] \quad \text{.....(4.23)}$$

and for the right AC side:

$$p_{2iac}^{abc} = v_{2i}^{abc} (i_2^{abc})^T = p_{2iac} = (P^{-1} v_{2i})(P^{-1} i_2)^T$$
$$= \frac{3}{2}[v_{2id} i_{2d} + v_{2iq} i_{2q} + 2 v_{2i0} i_{20}] \quad \text{.....(4.24)}$$

Then the currents i_{dc1} and i_{dc2} can be written as a function of the AC side variables as follows:

$$i_{dc1} = \frac{3[v_{1id} i_{1d} + v_{1iq} i_{1q}]}{2 v_{dc1}} \quad \text{.....(4.25)}$$

$$i_{dc2} = \frac{3[v_{2d} i_{1d} + v_{2iq} i_{1q}]}{2 v_{dc2}} \quad \text{.....(4.26)}$$

As the system is considered balanced, $i_{l0} = 0$ and $i_{20} = 0$.

Equations (4.25) and (4.26) can be substituted in (4.18) and (4.19), respectively. Then the whole model of the **AC-DC system** is composed by the equations (4.9), (4.10), (4.17), (4.18) and (4.19). This can be written in the state-space standard form:

$$\dot{x} = f(x,u) \quad \text{.....(4.27)}$$

$$x = [i_{1d} \quad i_{1q} \quad v_{dc1} \quad i_{dc12} \quad i_{2d} \quad i_{2q} \quad i_{2q}]^T \quad \text{.....(4.28)}$$

$$u = [\delta_1 \quad M_1 \quad \delta_2 \quad M_2]^T \quad \text{.....(4.29)}$$

CHAPTER 5
SIMULATION AND RESULTS

5.1 SYSTEM MODEL

The doubly fed induction generator based wind turbine is connected to the grid located 30 km as shown in Fig.5.1. The grid is further connected with 5MVA HVDC model through a step-up transformer stepping the voltage from 400V to 1600V. The converter operating as rectifier converts ac to dc voltage. The obtained dc output is connected to 200 km long transmission line to converter operating as inverter to yield ac. The Fig.5.1 shows the controls for both the rectifier and inverter converters. HVDC model represents the asynchronous link between the two converter stations. The filters are used to remove the ripples present in the ac voltage. Using a step down transformer (1000V to 500V) the voltage is observed at consumer end.

5.2 DFIG TURBINE MODEL

Wind turbines driven doubly-fed induction generator (DFIG) consist of a wound rotor induction generator and an AC/DC/AC IGBT-based PWM converter. The stator winding is connected directly to the 60 Hz grid while the rotor is fed at variable frequency through the AC/DC/AC converter as shown in Fig.5.2. This arrangement of DFIG control allows extracting maximum energy from the wind for low wind speeds by optimizing the turbine speed, while minimizing mechanical stresses on the turbine during gusts of wind. The optimum turbine speed producing maximum mechanical energy for a given wind speed is proportional to the wind speed as discussed in detail in Chapter 3. The system is modelled in SIMULINK and sub-blocks are discussed. They are-

- **Induction Generator Model**
- **Converter and Pitch Control Model**
- **Wind turbine Model**

5.2.1 INDUCTION GENERATOR MODEL

The electrical part of the machine is represented by a fourth-order state-space model and the mechanical part by a second-order system. The electrical variables and

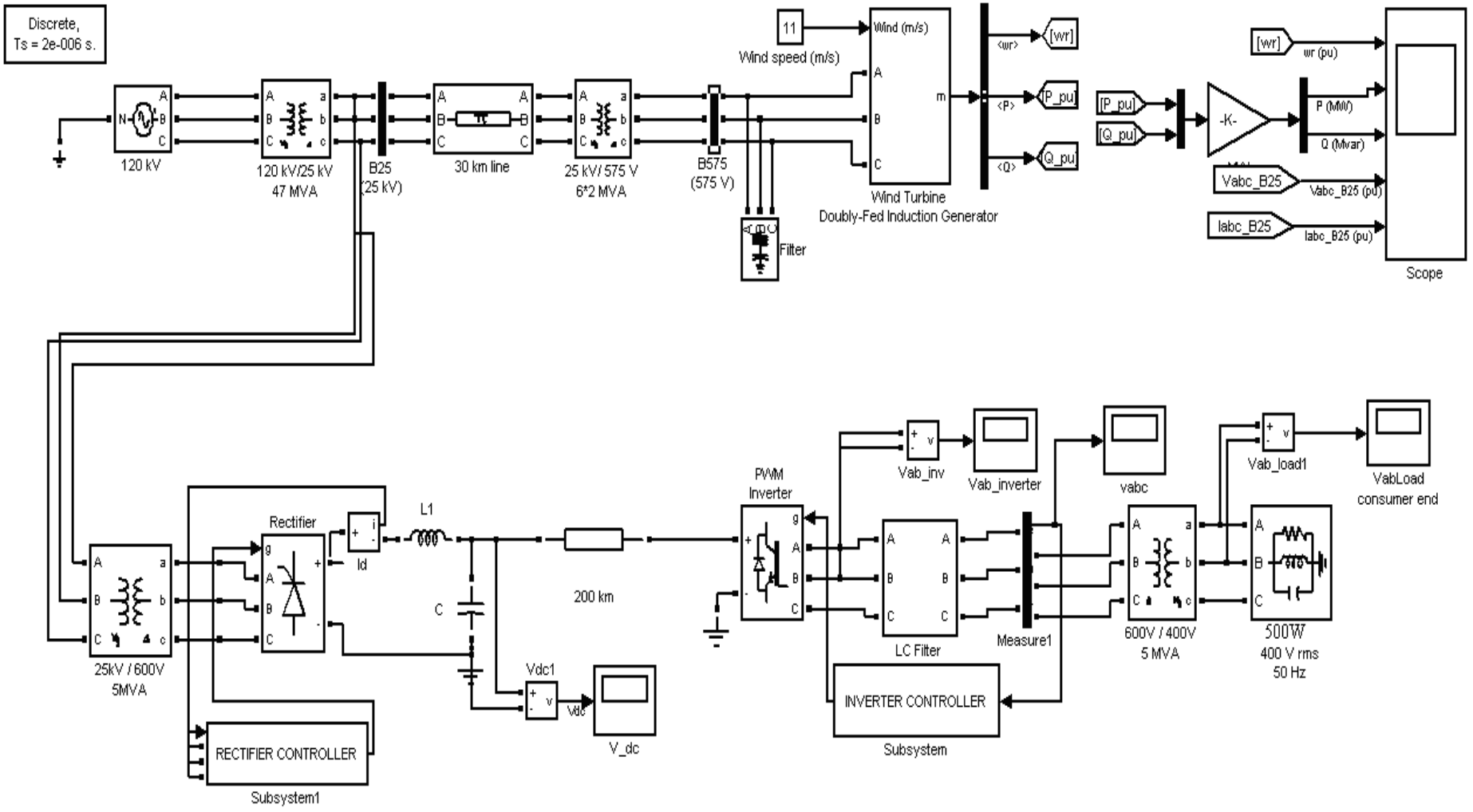

Fig. 5.1 System Model

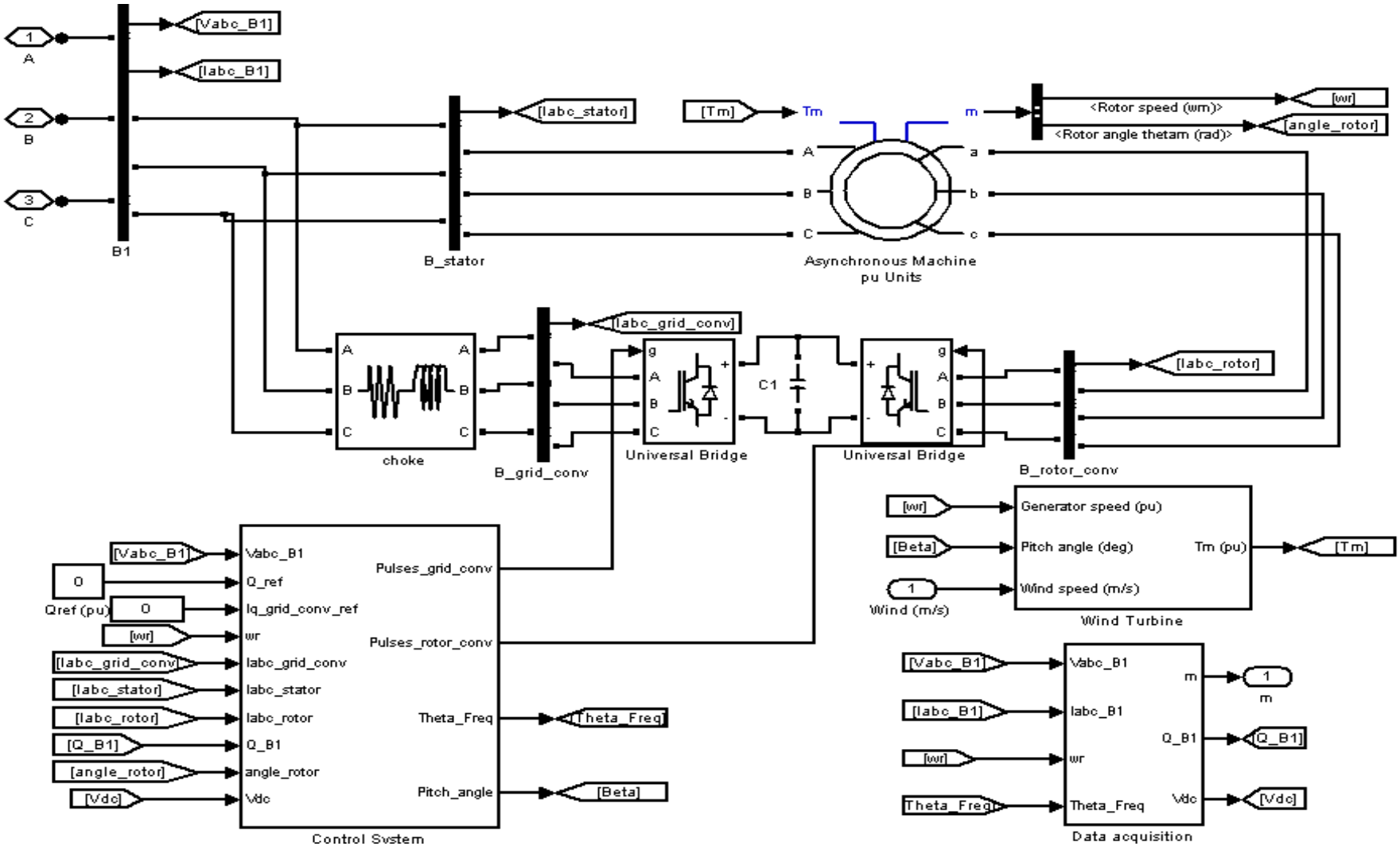

Fig.5.2 DFIG driven Wind turbine Model

parameters are referred to the stator. All stator and rotor quantities are in the arbitrary d-q axis reference frame (dq frame).

The electrical model suggests that the stator and rotor fluxes are obtained using the numerical integration from Eq. (3.14)-(3.17). However, the stator and rotor currents are obtained using the computed fluxes and the inductance parameters. Further, the above model is a d-q variable model and therefore the outcome will be d-q axes fluxes and currents. For the clarity, the dq variables are to be converted back into the phase variables. For computing the fluxes the stator and rotor voltages, which are the input, are to be represented into the dq variables. Therefore, the implementation is carried out using the following steps:

Step 1 The Vds, Vqs, Vdr, Vqr are obtained from the phase $_{\text{variables}}$ V^{s}_{abc} and V^{r}_{abc} through the following sub-steps:

- The sine and cosine values for Θ, ωr and β are calculated where,

  ωr is angular speed of rotor

  Θ is rotor angle

  And, β = Θ- Θr

- The stator & rotor voltages (V^{s}_{abc} , V^{r}_{abc}) are transformed into dq axes to form Vdqs and Vdqr using Park transformation to form equation no (3.7) to (3.10)

Step 2 The mutual fluxes for rotor and stator side can be calculated as shown in Fig.5.3.

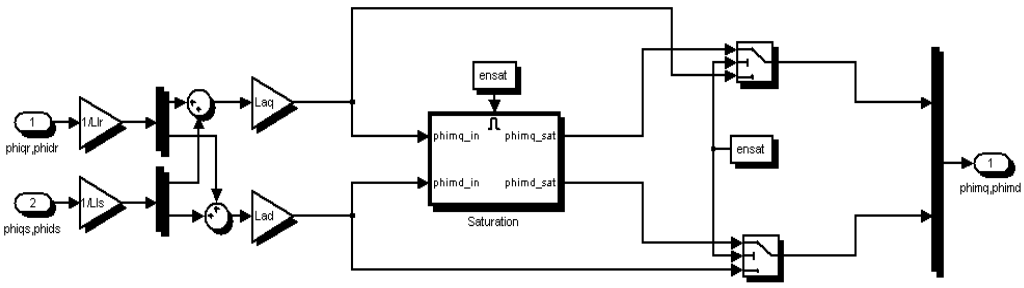

Fig.5.3 Mutual Flux Linkage of Asynchronous Machine

$$\varphi_{mq\_in} = \left(\frac{\varphi_{qr}}{L_{lr}} + \frac{\varphi_{qs}}{L_{ls}} \right) L_{aq} \quad \text{.....(5.1a)}$$

$$\varphi_{md\_in} = \left(\frac{\varphi_{dr}}{L_{lr}} + \frac{\varphi_{ds}}{L_{ls}} \right) L_{ad} \quad \text{.....(5.1b)}$$

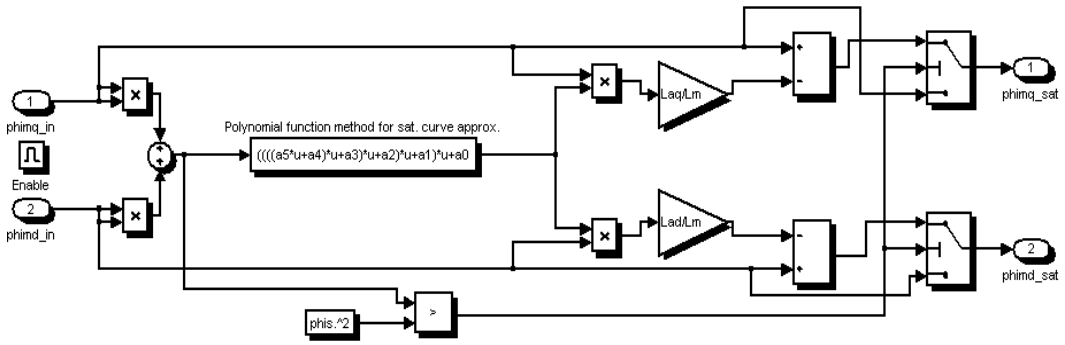

Fig.5.4 Subsystem of Mutual flux linkage (Saturation)

The mutual flux for the saturation that describes the magnetic saturation can be calculated from the Fig. 5.4 as the following:

$$\varphi_{mq\_sat} = \varphi_{mq\_in} - \left[(poly \quad func)\varphi_{mq\_in} \right] \frac{L_{aq}}{L_m} \quad \text{.....(5.2a)}$$

$$\varphi_{md\_sat} = \varphi_{md\_in} - \left[(poly \quad func)\varphi_{md\_in} \right] \frac{L_{ad}}{L_m} \quad \text{.....(5.2b)}$$

Step 3 The currents for stator and rotor side Idqs & Idqr are calculated as the following:

The current and flux equations for the **rotor side of induction generator** are modeled from Fig.5.5 as:

$$i_{qr} = k \ \varphi_{qr} - \varphi_{mq} \quad \text{.....(5.3a)}$$

$$i_{dr} = k \ \varphi_{dr} - \varphi_{md} \quad \text{.....(5.3b)}$$

$$\varphi_{qr} = k \ V_{qr} - \varphi_{dr}(\omega - \omega_r) i_{qr} \quad \text{.....(5.4a)}$$

$$\varphi_{dr} = k \ V_{dr} - \varphi_{qr}(\omega - \omega_r) i_{dr} \quad \text{.....(5.4b)}$$

Where φ_{md} and φ_{mq} are obtained in Eq no. (5.2a) and (5.2b)

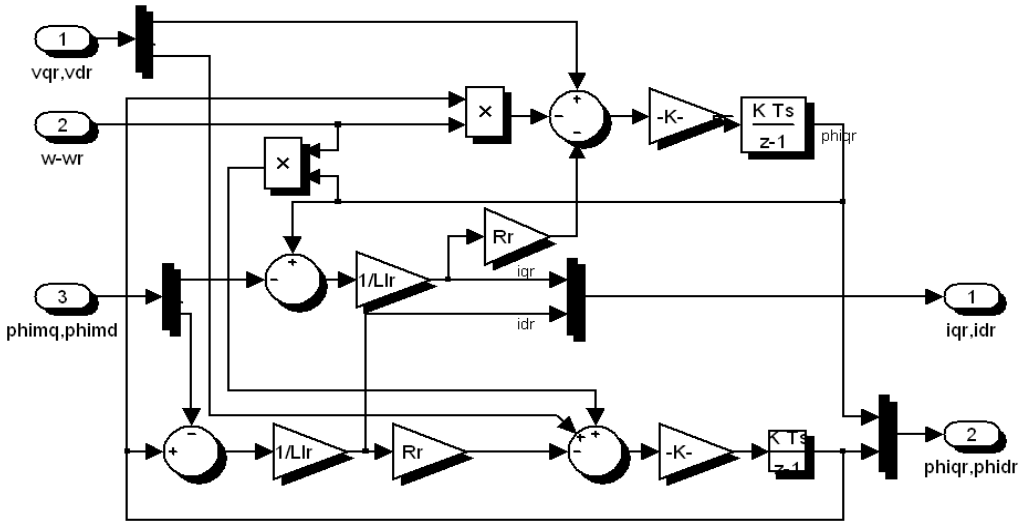

Fig.5.5 Model of Rotor side of Induction Generator

The current and flux equations for the **stator side of induction generator** as shown in Fig.5.6 are modelled as:

$$i_{qs} = k\ \ \varphi_{qs} - \varphi_{mq} \quad \text{.....(5.5a)}$$

$$i_{ds} = k\ \ \varphi_{ds} - \varphi_{md} \quad \text{.....(5.5b)}$$

$$\varphi_{qs} = k\ \ V_{qs} - \omega\varphi_{ds} - i_{qs} \quad \text{.....(5.6a)}$$

$$\varphi_{ds} = k\ \ V_{ds} - \omega\varphi_{qs} - i_{ds} \quad \text{.....(5.6b)}$$

$$\varphi_s = \sqrt{\varphi_{qs}^2 + \varphi_{ds}^2} \quad \text{.....(5.7)}$$

$$i_s = \sqrt{i_{qs}^2 + i_{ds}^2} \quad \text{.....(5.8)}$$

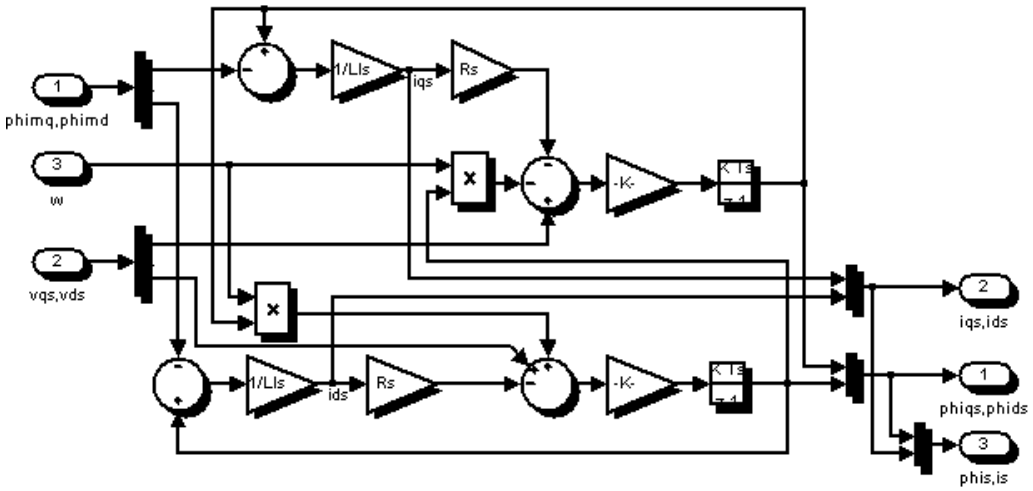

Fig.5.6. Model of Stator side of Induction Generator

Step 4: The rotor and stator side currents are transformed into phase currents.

Step 5: Torque is calculated as shown in above equation (3.13) from the Fig. 5.8.

Step 6: From the mechanical model of the induction generator equation (3.13b) is obtained.

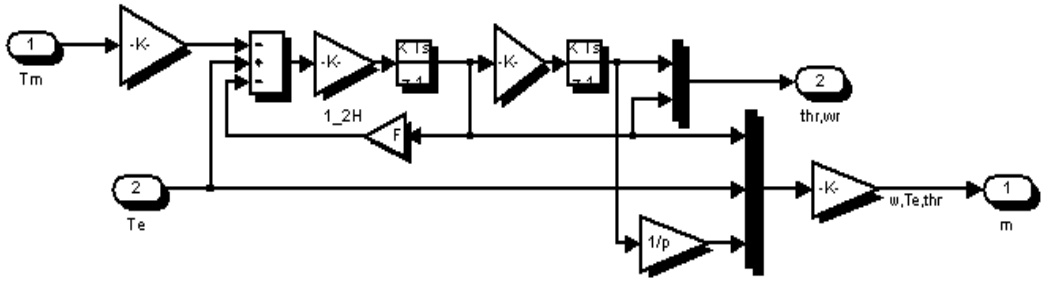

Fig.5.7. Mechanical Model of Induction Generator

Following equations are implemented to simulate the mechanical model as shown in Fig.5.7.

$$\frac{d\theta_r}{dt} = k\left(\frac{1}{2H}\right) T_e - T_m - \omega_r \quad \text{.....(5.9a)}$$

$$\omega_r = \left(\frac{1}{2H}\right) T_e - T_m - \omega_r \quad \text{.....(5.9b)}$$

The complete simulink model of Induction Generator constitutes to as shown below in Fig.5.8.

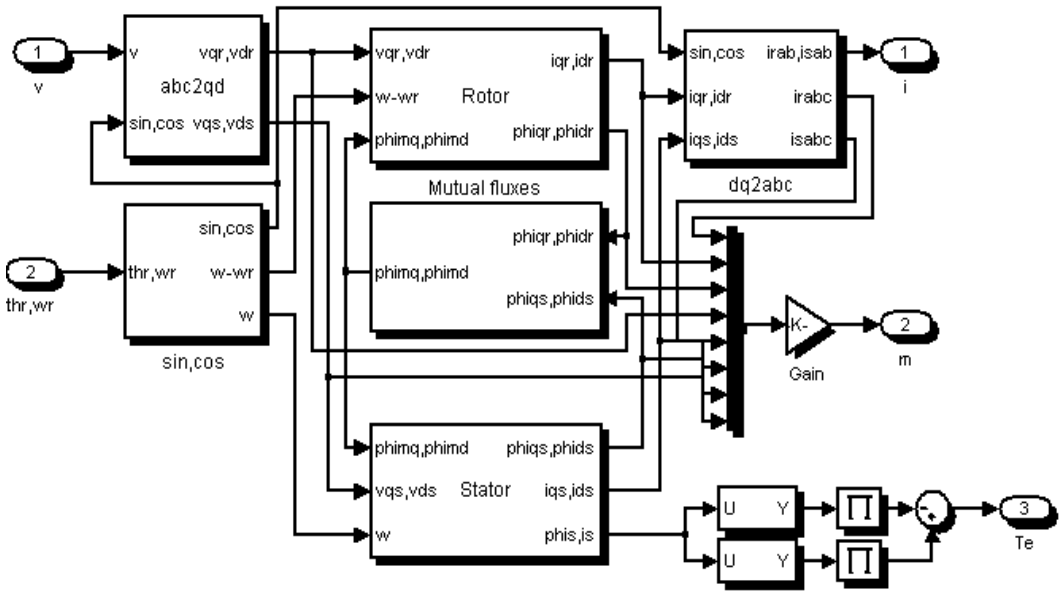

Fig.5.8 Model of Induction Generator

5.2.2 CONVERTER AND PITCH CONTROL MODEL

The control sub-system shown in Fig.5.2 is represented in expanded form in Fig.5.9. It consists of: filter block, control block for grid side controller and rotor side controller and PWM generator for both the IGBT converters.

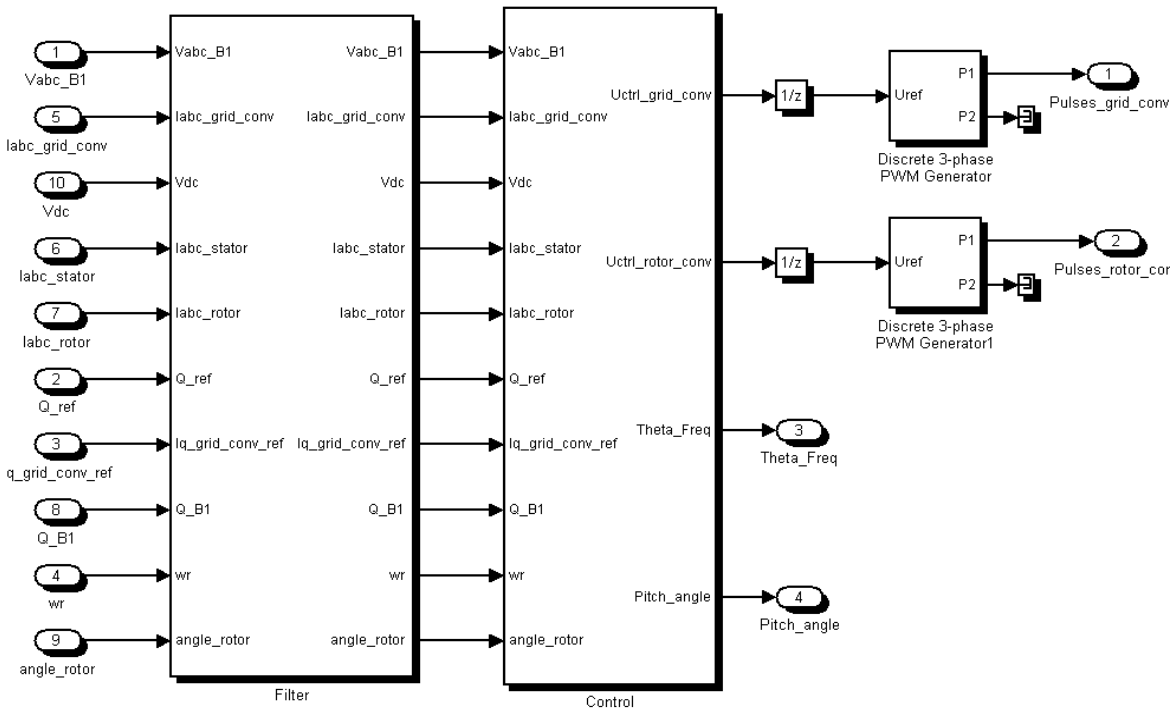

Fig.5.9 Subsystem of control system

The 'filter' block in Fig.5.9 represents the Discrete Second order filters are used to reduce or enhance certain aspects of the signal, having cut off frequency of 1000Hz and damping factor of 0.707. The Model of Control System can be studied under four sub-models as shown in Fig.5.10. These sub-models are-

- **Discrete Phase Locked Loop**
- **Grid Side Converter control**
- **Rotor Side Converter Control**
- **Pitch angle control**

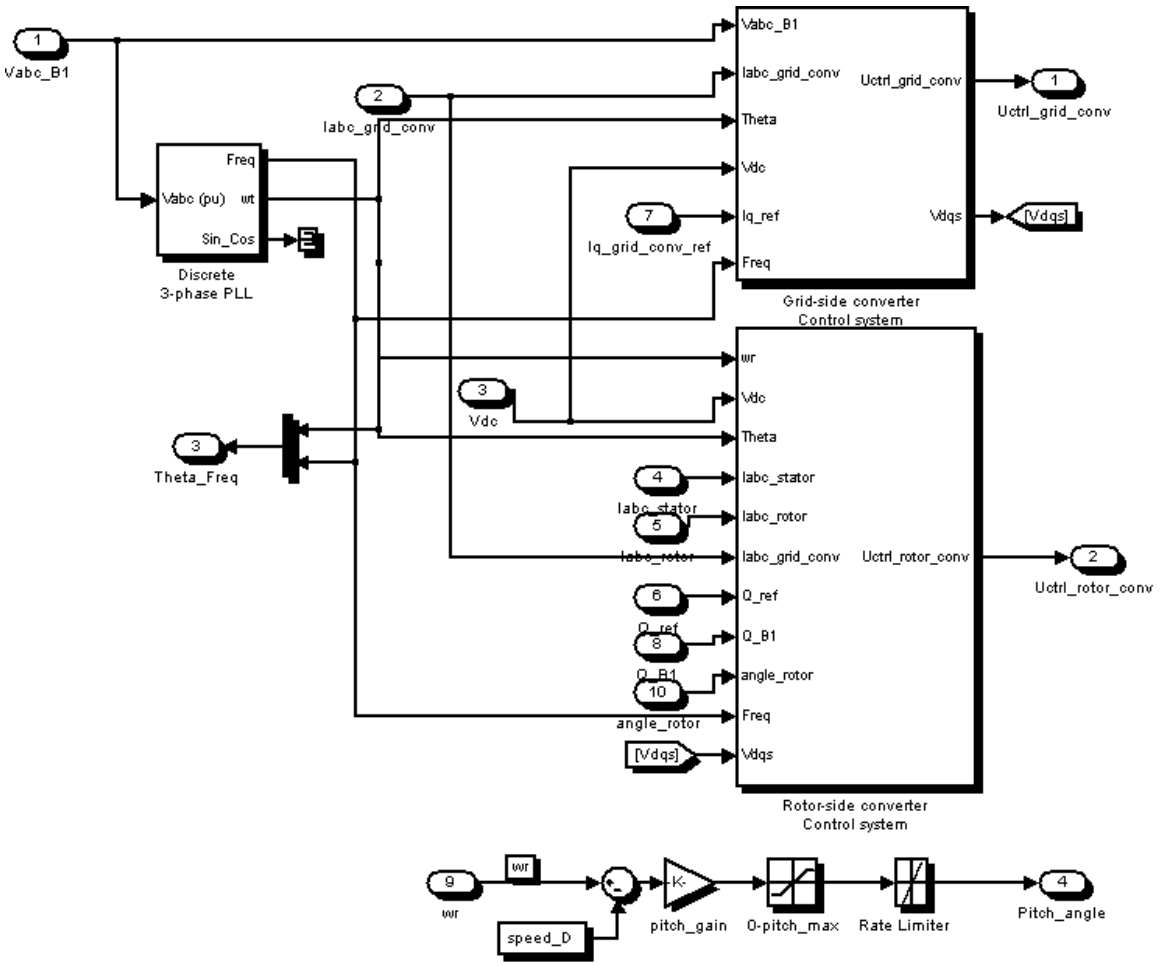

Fig.5.10 Subsystem of control block

A **Discrete phase-locked loop** is a control system that tries to generate an output signal whose phase is related to the phase of the input "reference" signal. This circuit compares the phase of the input signal with the phase of the signal derived from its output oscillator and adjusts the frequency of its oscillator to keep the phases matched. Phase locked loop system is used to synchronize on a set of variable frequency, three phase sinusoidal signals. This 'Discrete 3-phase PLL' has three inputs and two output signals defined as-

Input: Three phase voltage signals [Va, Vb, Vc]

Output 1: Measured frequency [Hz] = $\frac{\omega}{2\pi}$

Output 2: Phase varying ωt from 0 to 2pi.

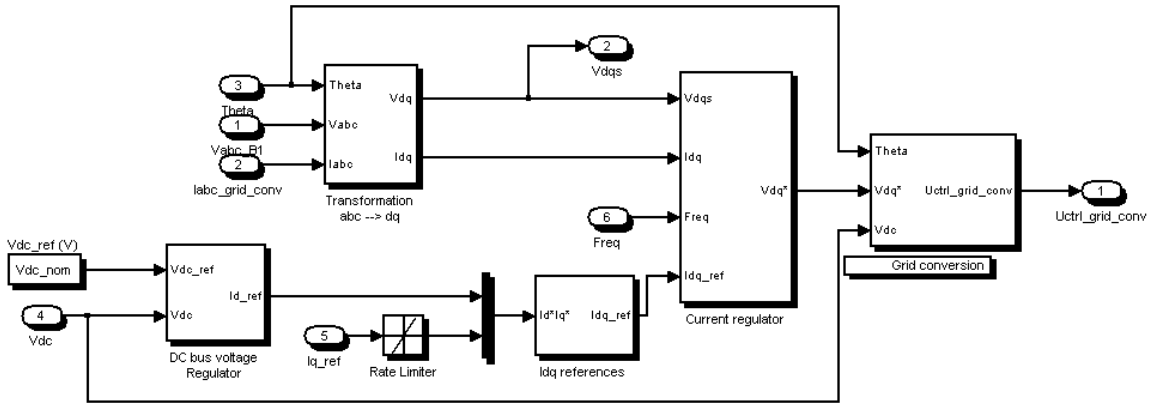

Fig.5.11 Grid side converter control system

The **grid side converter control** is shown in Fig.5.11. It is used to regulate the voltage of the DC bus capacitor. In addition, this model allows generation or absorption of reactive power. The operation is explained as the following:

- Transforming the voltages and currents Vabcs and Iabcs into dq reference frame.
- An outer regulation loop consists of a DC voltage regulator. It computes the output reference current Id_ref between the nominal DC voltage and DC voltage, for the current regulator (Id_ref = current in phase with grid voltage which controls active power flow).
- An inner current regulation loop consisting of a current regulator. The current regulator controls the magnitude and phase of the voltage generated by converter control grid from the Id_ref produced by the DC voltage regulator and specified Idq_ref reference. The current regulator is assisted by feed forward terms which predict the Control grid output voltage. The magnitude of the reference grid converter current is given by:

$$I_{gc\_ref} = \sqrt{I_{d\_ref}^2 - I_{q\_ref}^2}$$

The maximum value of this current is limited to a value defined by the converter maximum power at nominal voltage. The stator voltage obtained is delayed by one step and provided to PWM generator. The PWM generated pulses control the stator side converter.

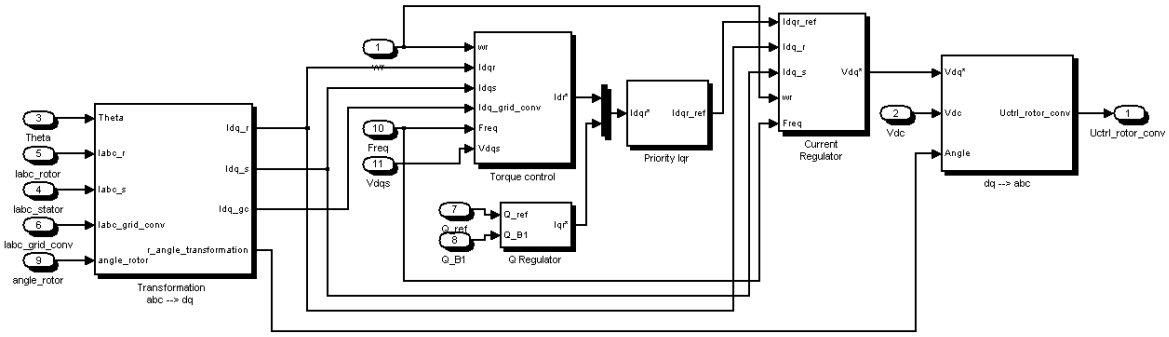

Fig.5.12 Rotor side converter control system

The voltage or the reactive power at grid terminals is controlled by the reactive current flowing in the rotor converter. **Rotor-Side Converter Control System** is shown in Fig.5.12. It consists of-

- Transforming the currents of stator, rotor and grid converter into dq reference frame such as Idq_r, Idq_s and Idq_gc.

- The actual electrical output power, measured at the grid terminals of the wind turbine, is added to the total power losses (mechanical and electrical) and is compared with the reference power. A Proportional-Integral (PI) regulator is used to reduce the power error to zero. Using the torque regulator the Idr_ref is calculated.

- The output of reactive regulator 'Q Regulator' is the reference rotor current Iqr_ref that must be injected in the rotor converter.

- The actual Iqr component of positive-sequence current is compared to Iqr_ref and the error is reduced to zero by a current regulator (PI). The output of this current controller is the voltage Vqr generated by rotor converter. The current regulator is assisted by feed forward terms which predict Vqr.

- Voltage at the rotor converter Vdqr is transformed into abc reference frame.

The rotor voltage obtained is delayed by one step and provided to PWM generator. The PWM generated pulses controls the rotor side converter.

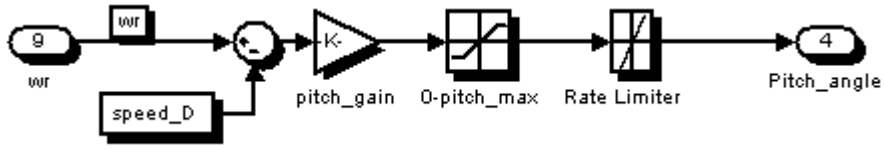

Fig.5.13 Pitch angle controller

Pitch_angle = ω_r – Speed_D

The value of Speed_D is 1.21pu.

Wind turbine is designed to produce optimum power with 11 m/s of wind speed. However, the wind speed always fluctuates up and down around this optimum. To generate the optimum power, **pitch** needs to be controlled.

The PWM Generator block generates pulses for carrier-based pulse width modulation (PWM) converter using two-level topology. The block can be used to fire the forced-commutated devices IGBTs. The pulses are generated by comparing a triangular carrier waveform to a reference modulating signal. The modulating signals can be generated by the PWM generator itself, or they can be a vector of external signals connected at the input of the block. The amplitude (modulation), phase, and frequency of the reference signals are set to control the output voltage (on the AC terminals) of the bridge connected to the PWM Generator block.

5.2.3 WIND TURBINE MODEL

The wind turbine model is based on the steady-state power characteristics of the turbine as shown in Fig.5.14. The stiffness of the drive train is infinite and the friction factor and the inertia of the turbine must be combined with those of the generator coupled to the turbine. The output power of the turbine is given by the following equation.

$$P_{mech} = 0.5 C_p \rho_{air} \pi R^2 V_{wind}^3 \quad \text{.....(5.10)}$$

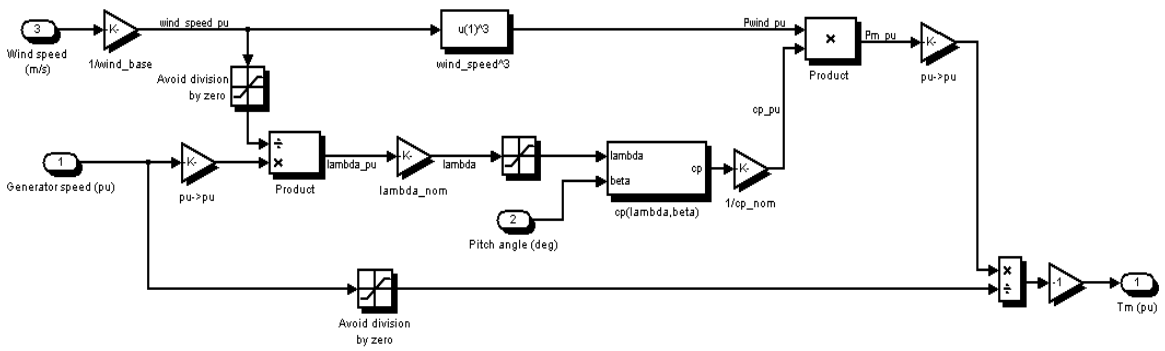

Fig.5.14 Modeling of Wind turbine

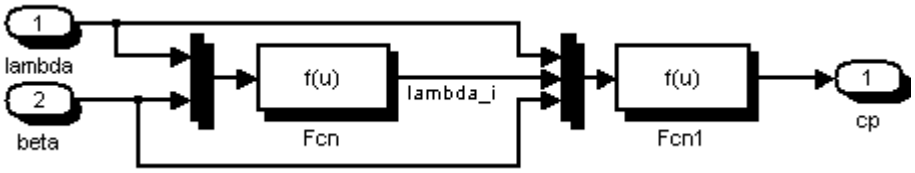

Fig.5.15 Cp calculation

The rotations or speed of wind turbine is controlled by pitch control during the varying wind. The pitch control thus extracts a fraction of the power in the wind. This fraction is expressed as the power efficiency coefficient, Cp, of the wind turbine as shown in figure 5.15. The Cp can be expressed as a function of λ and β:

$$C_p = f(\lambda, \beta) \quad \text{.....(5.11)}$$

5.3 HVDC SYSTEM MODEL

The output generation power from wind turbine is connected to HVDC System. Using the rectifier the AC voltage is converted into DC voltage. The filtered DC voltage is applied to an IGBT inverter generating 50 Hz. The IGBT inverter uses Pulse Width Modulation. The load voltage is regulated at 1 pu (1000V rms) by a PI voltage regulator using abc to dq and dq to abc transformations. The first output of the voltage regulator is a vector containing the three modulating signals used by the PMW Generator to generate the 6 IGBT pulses. The second output returns the modulation index. Using LC filters the voltage is observed at the consumer end. The HVDC System is shown in Fig.5.1

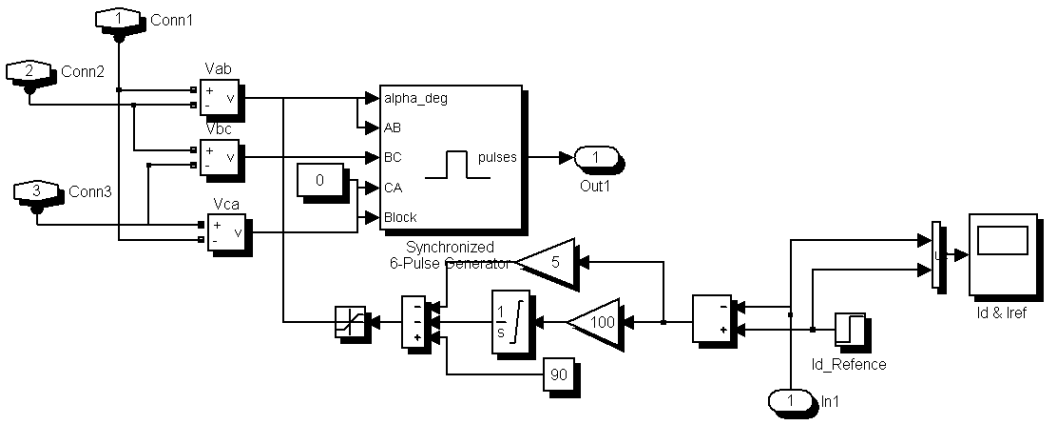

Fig.5.16 Subsystem of Rectifier control

A pulse generator synchronized on the source voltages provides the trigger pulses for the six thyristors. The converter output current is controlled by a PI current regulator built with Simulink blocks as shown in Fig.5.16. A step signal is applied to the reference input to test the dynamic response of the current regulator.

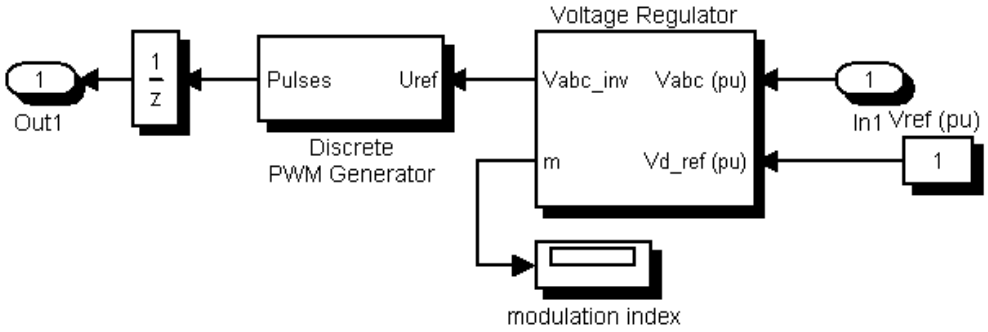

Fig.5.17 Simulated PWM Discrete Pulse Generation for Inverter

The rectified dc is then made to pass through a DC link. From, the DC link, the dc voltage is transmitted via a long distance HVDC line. At the inverter station, the transmitted dc voltage is inverted to get the ac voltage. The inverter uses PWM modulation to get the sinusoidal waveform. The control system of inverter is shown in Fig.5.17.

The ac voltage obtained from inverter is then filtered by a system of filters comprising of inductors and capacitors. A filter system is shown in Fig.5.18. The filtered output is available at consumer end.

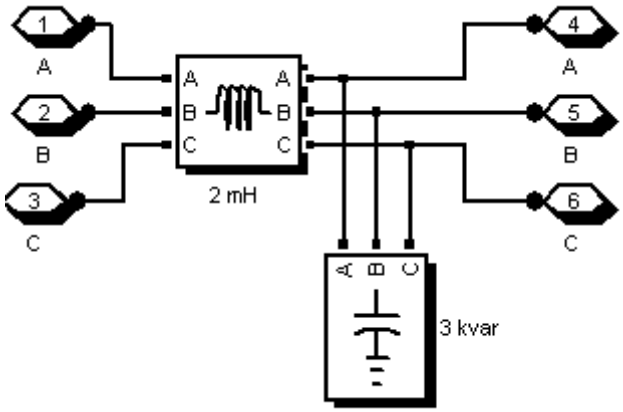

Fig.5.18 Filter System.

5.4 RESULTS AND DISCUSSIONS

The development of dynamic models of various components has been discussed in Chapter 3 and 4. The system model developed in SIMULINK environment is shown in Fig. 5.1. The model equations are solved by trapezoidal rule. The performance of the wind turbine driven DFIG system has been carried out through the following two case studies.

Case I : The performance of DFIG with HVDC system.

Case II : The performance of DFIG without HVDC system.

The data of various simulated models are given in Appendix. The turbine power characteristics are shown in Fig. 5.19. As shown in Fig. 5.19, different curves, which are obtained for different base speeds, represent the variation between turbine output power for turbine speed. It is observed that the mechanical power output increases with the increase in wind speed non-linearly upto a speed after which it starts reducing. The optimum turbine speed producing maximum mechanical energy for a given wind speed is proportional to the wind speed. For the base speed of 11m/sec, the maximum mechanical output power is observed 0.75pu at 1.2. pu turbine speed.

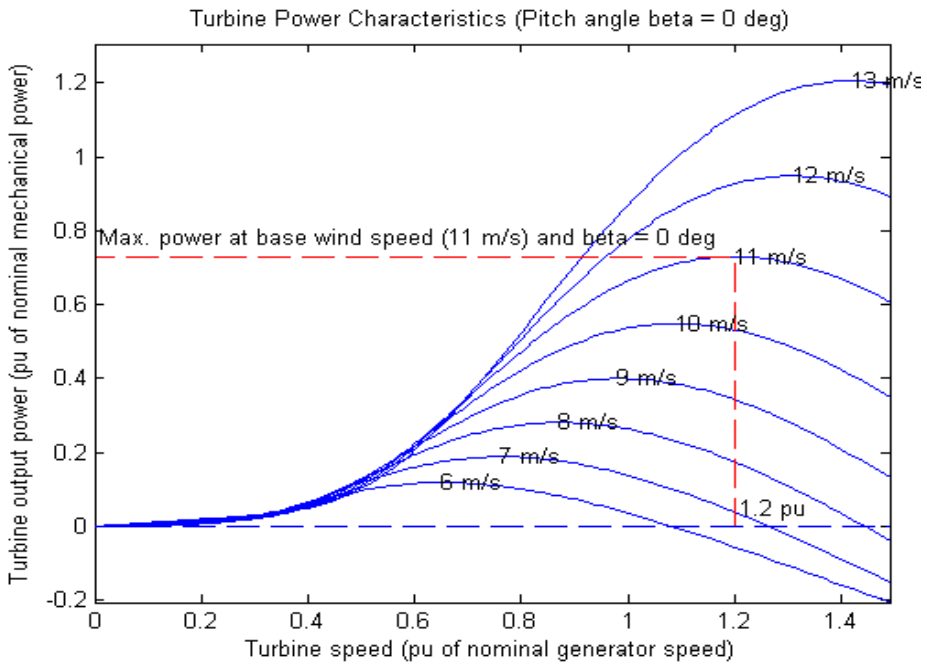

Fig.5.19 Represents Turbine Power Characteristics

5.4.1 PERFORMANCE OF DFIG WITH HVDC SYSTEM

The 9-MW wind farm comprises of six 1.5-MW wind turbines connected in parallel to a 25kV AC bus through a transmission line (30 km long) as shown in Fig.5.1. The doubly-fed induction generator (DFIG) consists of a wound rotor induction generator and an AC/DC/AC IGBT-based PWM converter. Each of the 3-phase induction generator is rated with line to line voltage of 575V, frequency 60Hz. The equivalent generation has nominal base as 10MVA, having inertia constant of 5.04 seconds and friction factor 0.01pu. The stator winding is connected directly to the 60 Hz grid while the rotor is fed at variable frequency through the AC/DC/AC converter. The DFIG technology allows extracting maximum energy from the wind for low wind speeds by regulating the turbine speed, while minimizing mechanical stresses on the turbine during gusts of wind. The output of generation available with wind farm DFIG is supplied to other loads connected through 5MVA HVDC transmission system consisting of (200km long) DC line.

For the simulation run the base wind speed is taken as 11m/s, the active power, the reactive power required by the DFIG, speed of wind turbine, voltage and current at 25 kV bus B25 is shown in Fig.5.20

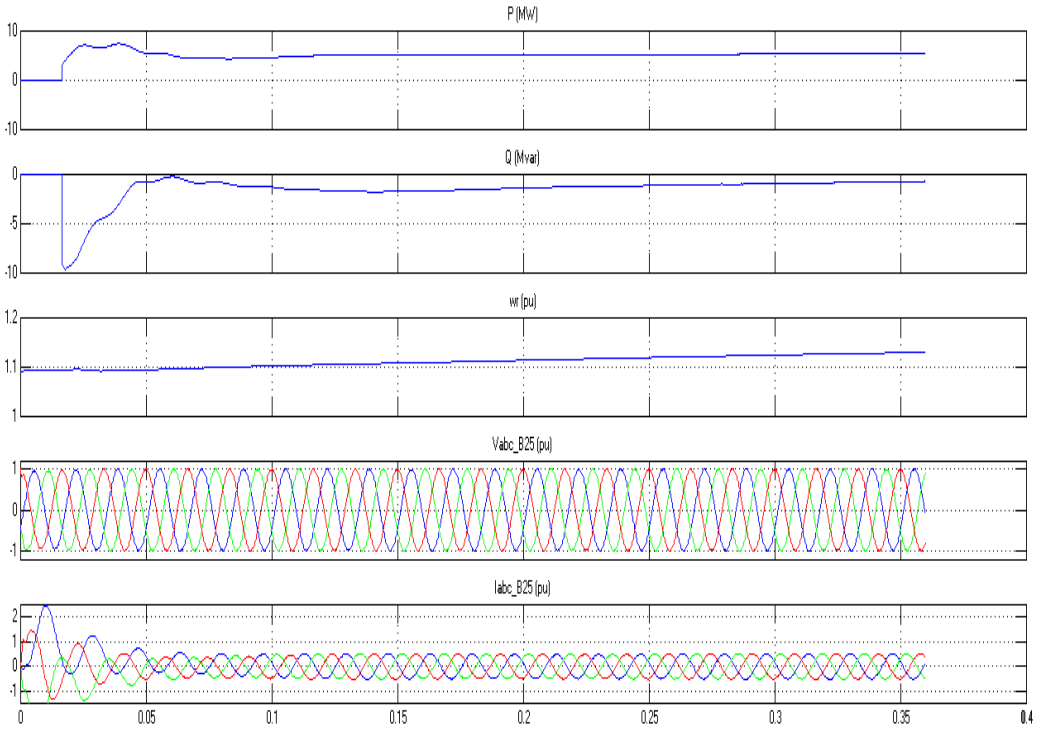

Fig.5.20 Wind Farm connected with HVDC System

The active power generated by the doubly fed induction generator increases momentarily to 7MW and afterwards decreases to steady state value of 5MW. This active power corresponds to the maximum mechanical turbine output for 11m/s base wind speed minus electrical and mechanical losses in the generator.

There is an excessive demand of reactive power momentarily to 9Mvar which reduces to 1Mvar after 0.35 seconds. The reactive power is managed by the filters and AC source. During this the dc link capacitor voltage is maintained constant by the converter. The turbine speed is maintained slightly higher than 1.1pu but lowers to 1.2pu. Because of it the extracted power is less than 0.75pu, the maximum extractable power.

The Grid voltage observed at the AC bus B25 is 1 pu in time period of 360ms. The current at the grid has a value of 0.5pu at AC bus B25. This value is attained after initial transients of decreasing magnitude.

The output of generated power from wind turbine is connected with 5MVA HVDC transmission system. For the simulation run, the rectified DC voltage, PWM inverter voltage, single phase and three phase voltages at the consumer end are shown in Fig. 5.21, Fig.5.22, Fig.5.23, and Fig.5.24 respectively.

The rectified DC voltage first increases to 1250V instantly and than achieve a steady state value of 800V. The DC line is characterized by the parameters such as length of 200km, capacitance of 0.004uF, inductance of 0.2uH and resistance of 0.015 ohms. The voltage is converted to AC using a PWM IGBT converter.

The LC filter is used for reducing the ripple content or the harmonics present in sinusoidal voltage, having inductance of 2mH and capacitance giving reactive power of 3kvar. The filtered voltage is stepped down by transformer to 600/400V. The single phase waveform shows constant value of 390 Volts throughout after the period of 0.05 seconds.

The 3 phase AC voltage waveform at the consumer end shows the same nature as the inverted waveform. The waveform is sinusoidal nature as expected of. It shows steady value of 230 volts.

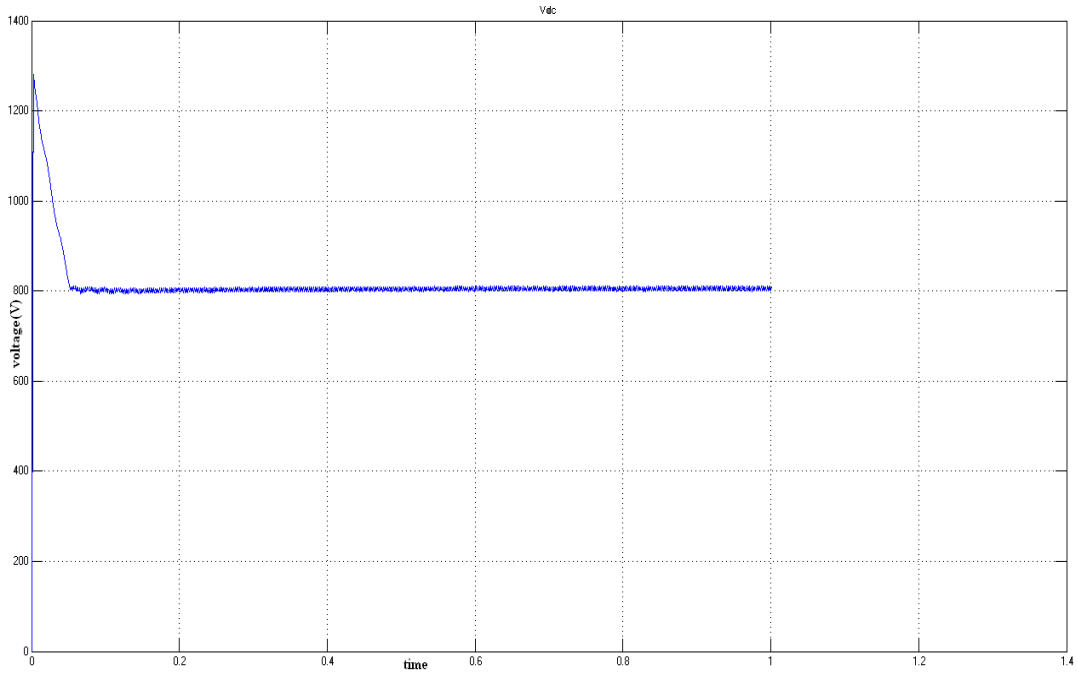

Fig.5.21 Rectified DC Voltage

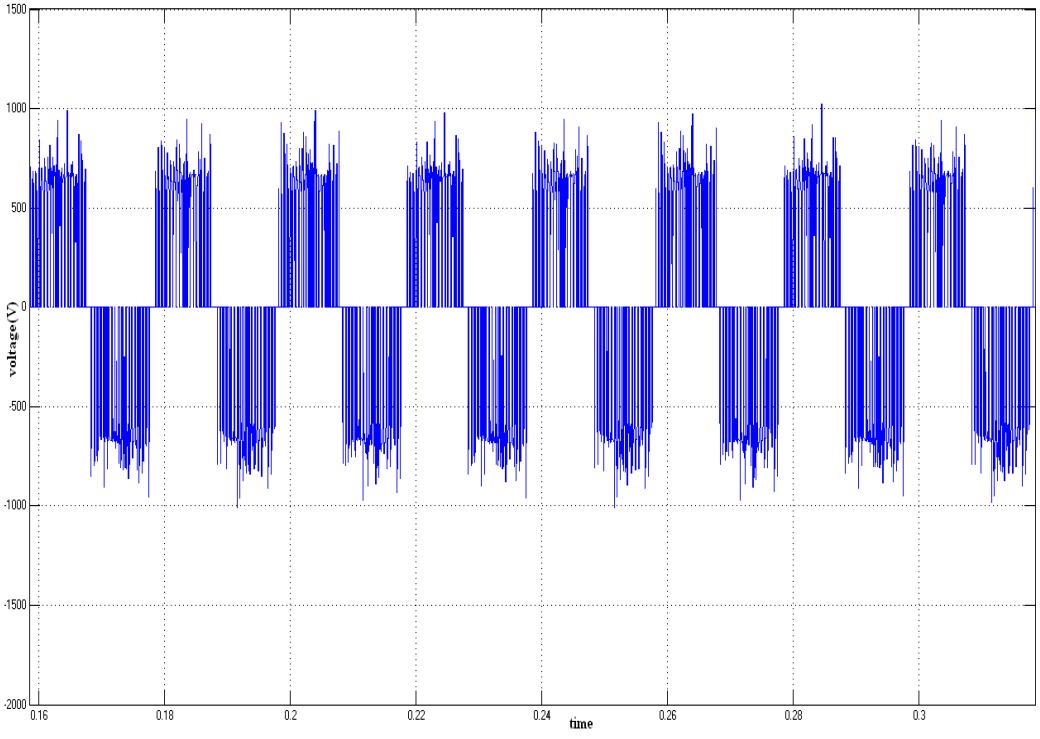

Fig.5.22 PWM Inverter Voltage

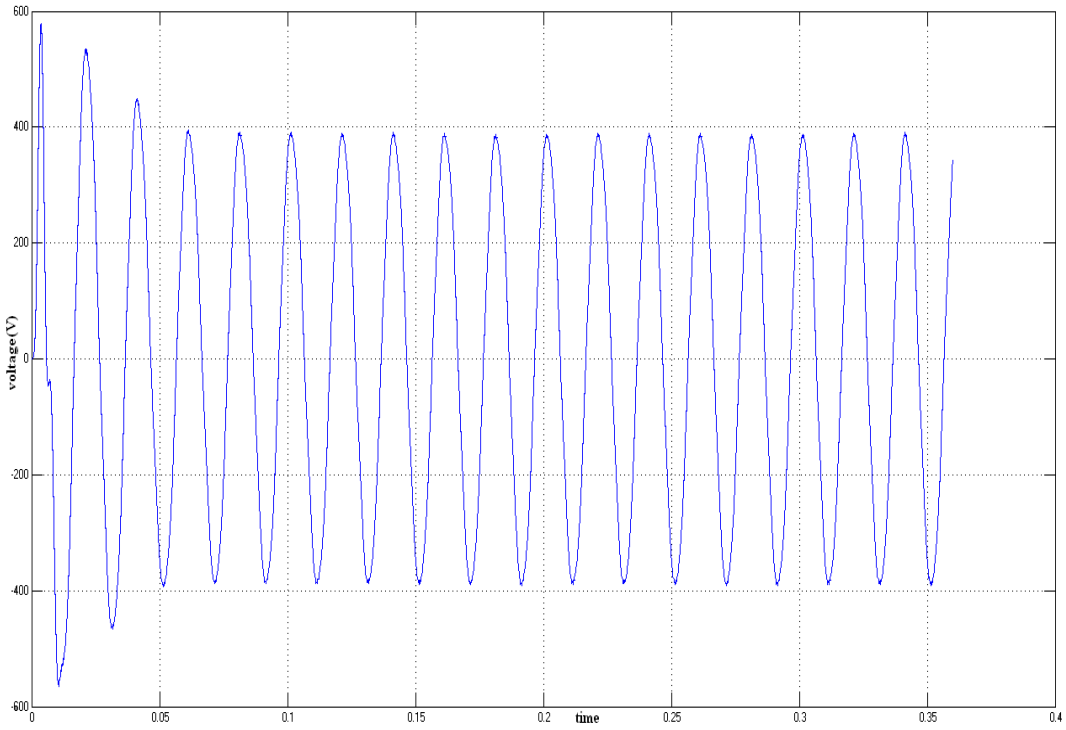

(a)Voltage Waveform

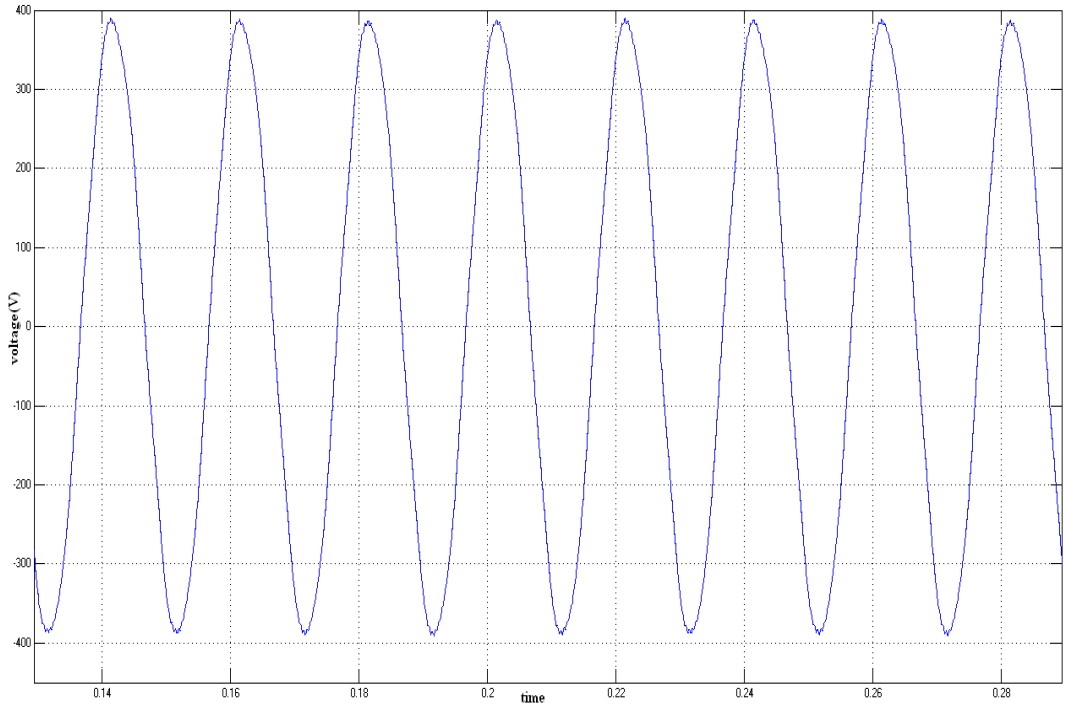

(b)Expanded View of Waveform

Fig.5.23 (a), (b) Single Phase AC Voltage Waveform

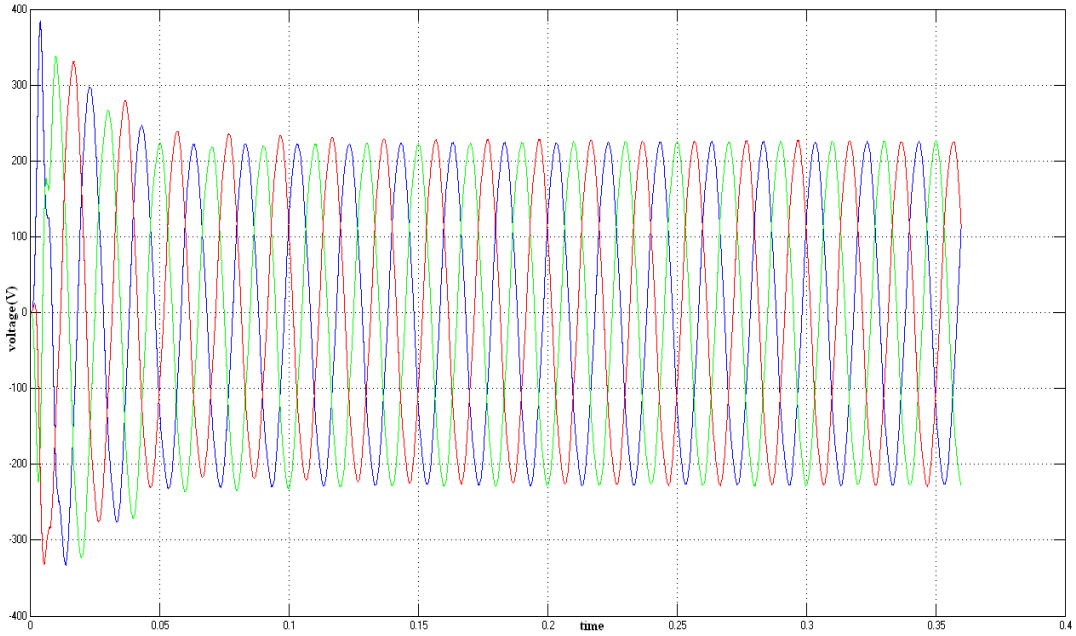

(a) Voltage Waveform

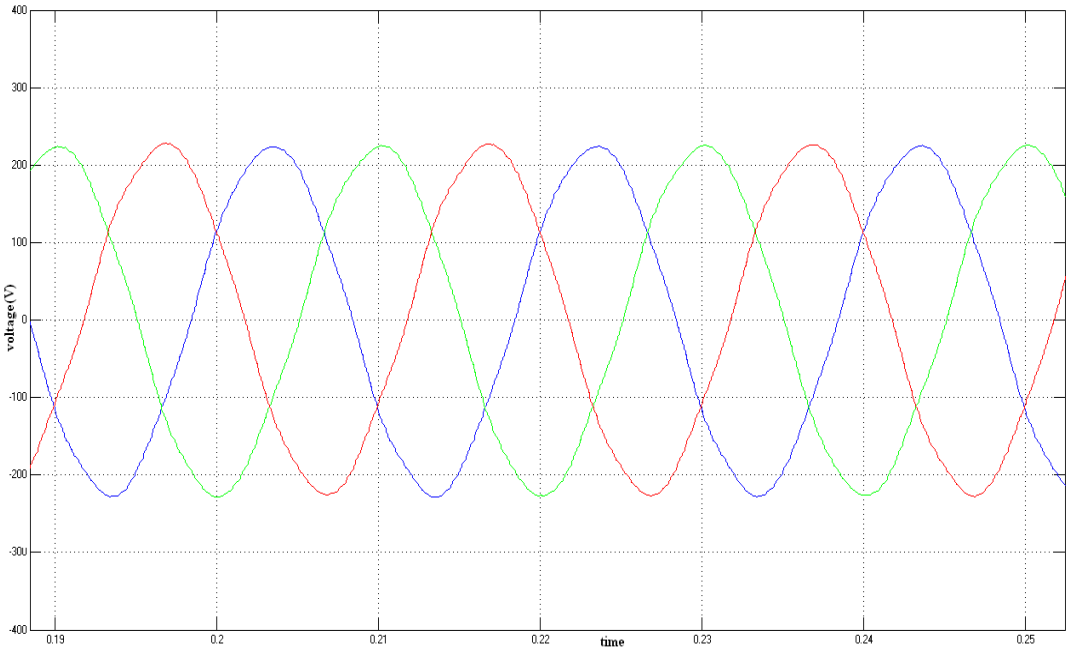

(b) Expanded View

Fig.5.24 (a),(b) Three Phase AC Voltage Waveform

(i) EFFECT OF CHANGE IN DC LINE LENGTH

The effect of change in DC line parameters is shown in Fig.5.25. As the parameters are expressed in per unit length, the length of the line is changed. The Fig.5.25 represents the single phase consumer end voltage for three line lengths which are 200km, 350km and 500km. DC line of length 200km long shows voltage of 390V as represented by waveform

1. For 350km line, voltage decreases to 360V as shown by waveform 2. For 500km line length, the voltage of 320V is resulted. The voltage drop results into lower voltage at consumer end. This also results into higher losses.

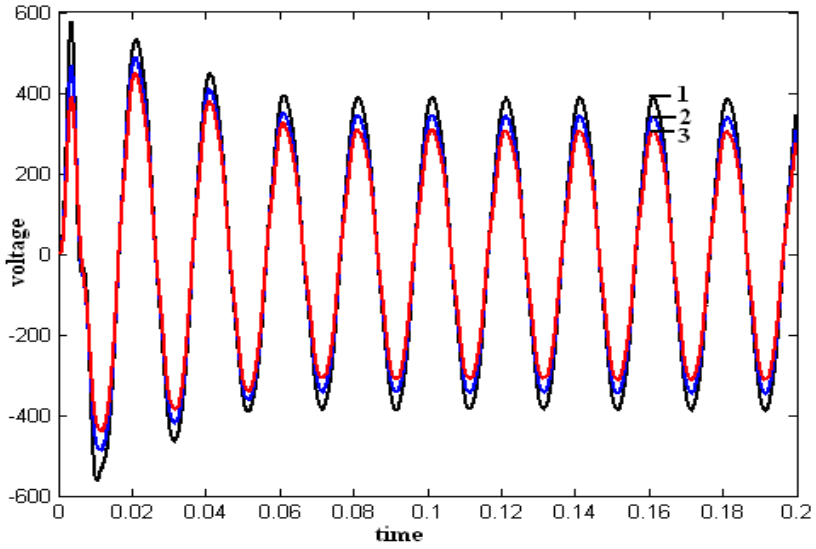

Fig.5.25 Effect Of Change in Dc Line Length

(ii) EFFECT OF CHANGE IN CONSUMER LOAD

This effect is shown in Fig.5.26.At no loading at the consumer end, as shown in waveform 1, the single phase voltage of 390V is resulted. On increasing the load to 50kW, keeping the other parameter constant, the voltage decreases to 350V as shown in waveform 2. Further, increase may result in further decrease in consumer voltage.

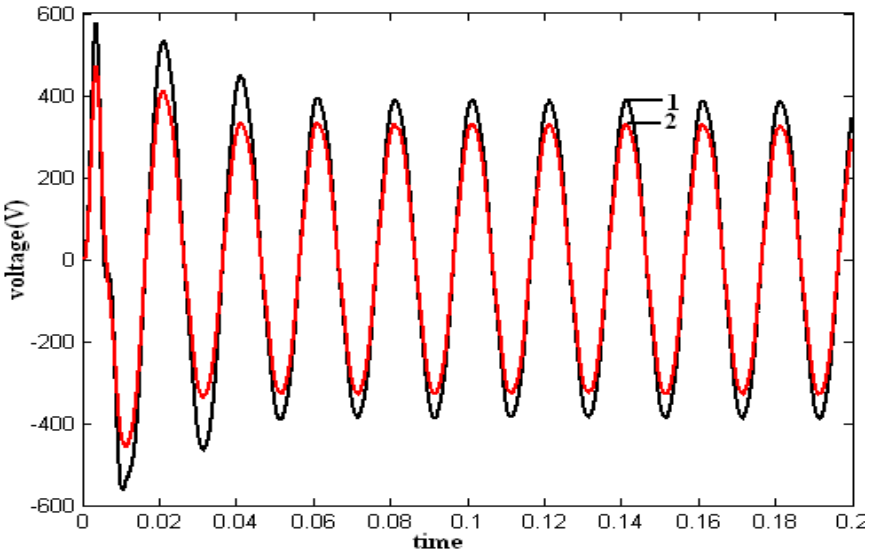

Fig.5.26 Effect Of Change In Consumer Load

(iii) EFFECT OF CHANGE IN GRID VOLTAGE

On changing the grid voltage to ± 10%, the single phase voltage and three phase voltage waveforms observed at consumer end are shown in Fig.27(a),(b) and Fig.28(a),(b). On decreasing the grid voltage to 108kV the voltage at consumer end decreases to 360V and on increasing the grid voltage to 132kV the voltage observed is 420V. Therefore, consumer voltage is directly related to AC bus voltage.

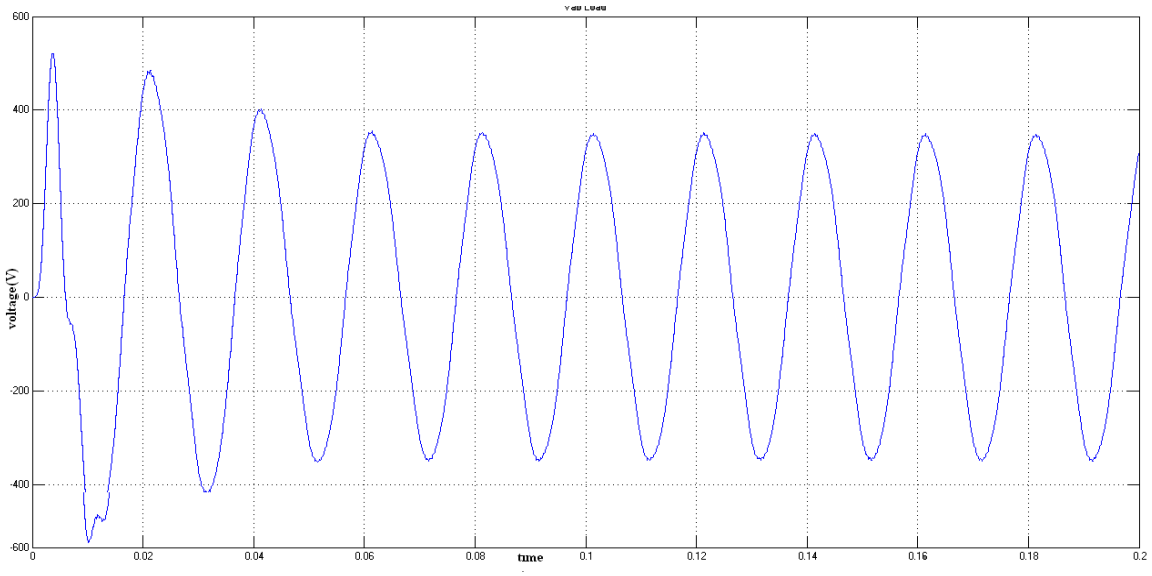

(a)

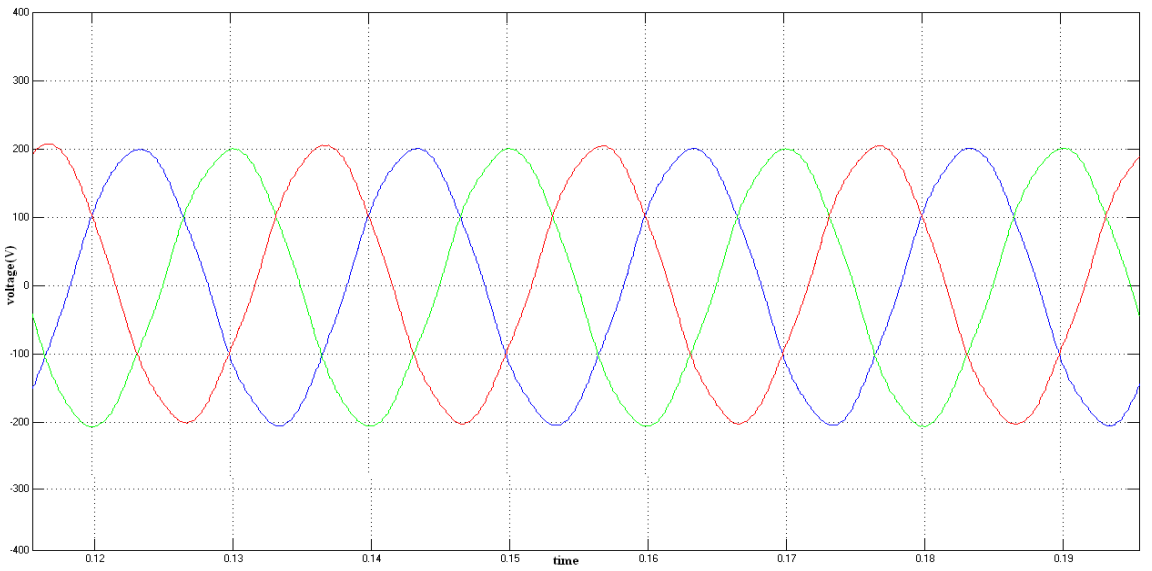

(b)

Fig.27(a),(b) Waveform observed at Grid Voltage of 108kV

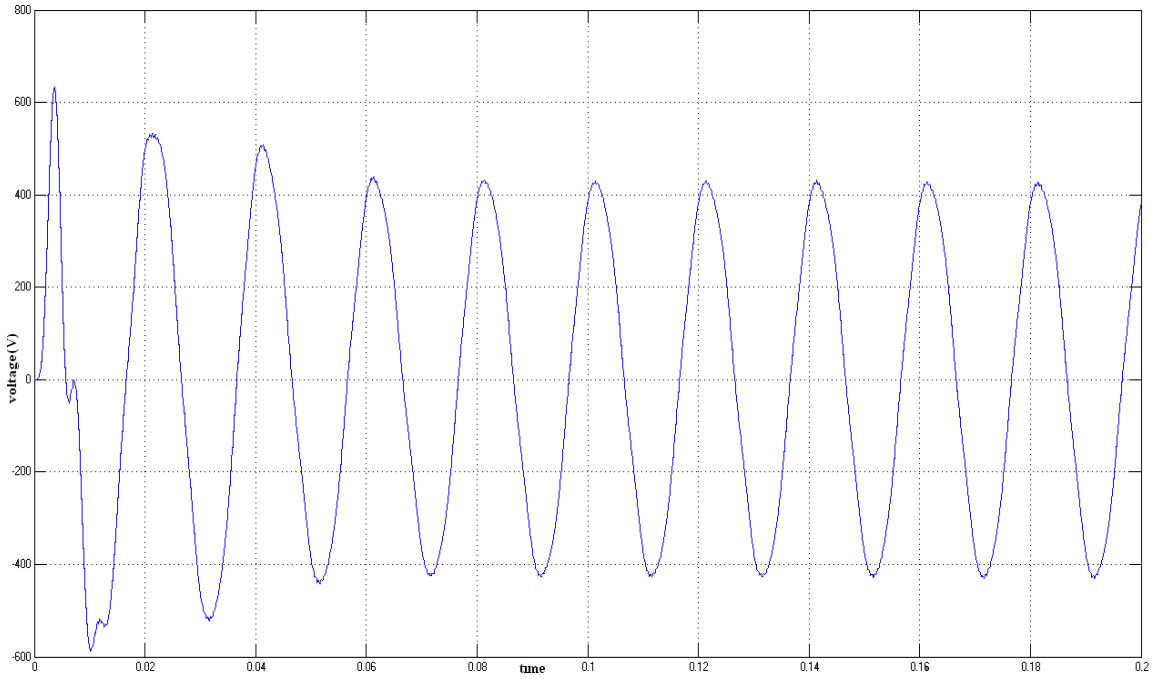

(a)

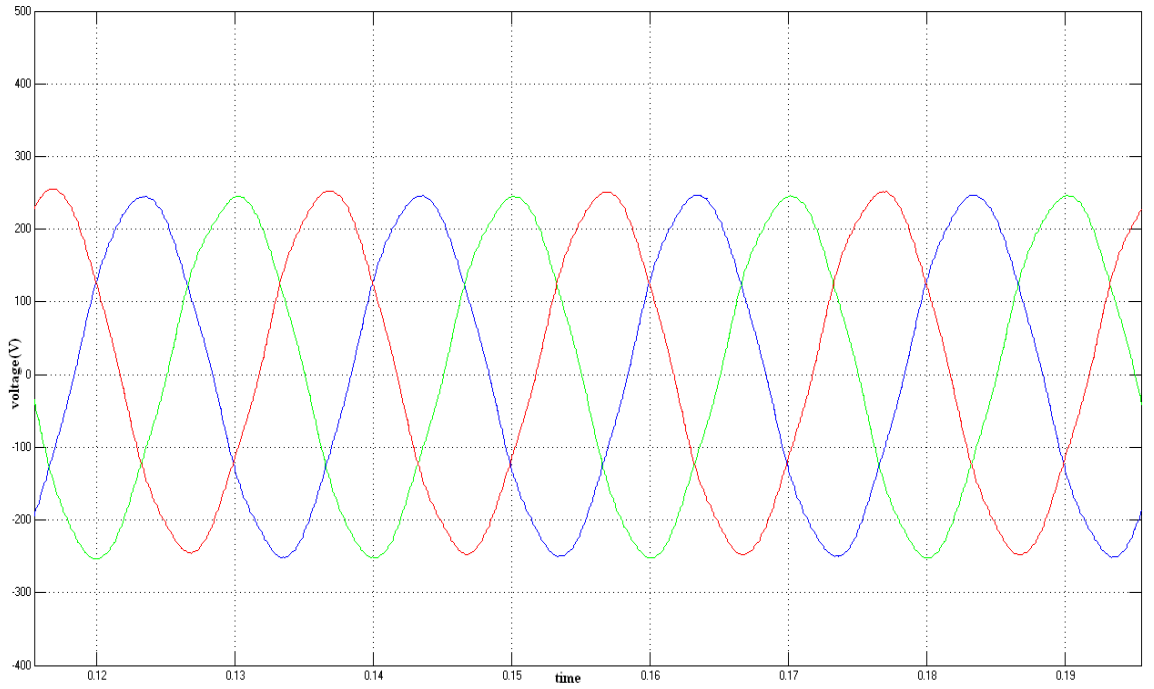

(b)

Fig.5.28 (a),(b) Waveform observed at Grid Voltage of 132kV

5.4.2 PERFORMANCE OF DFIG TURBINE WITHOUT CONNECTING HVDC SYSTEM

DFIG driven wind farm produces 5 MW when not connected with HVDC System. This active power corresponds to the maximum mechanical turbine output for a 11m/s wind speed minus electrical and mechanical losses in the generator. The corresponding turbine speed is 1.1 pu. The control system uses a torque controller in order to maintain the speed at 1.1 pu. The grid voltage of 1 pu and current of 0.5pu is observed as shown in Fig.29. For this the characteristics are similar to as shown in Fig.5.20, except the variation in turbine speed. In this turbine speed remains largely constant to 1.1 pu, whereas with HVDC, it increases and lies between 1.1pu and 1.2pu

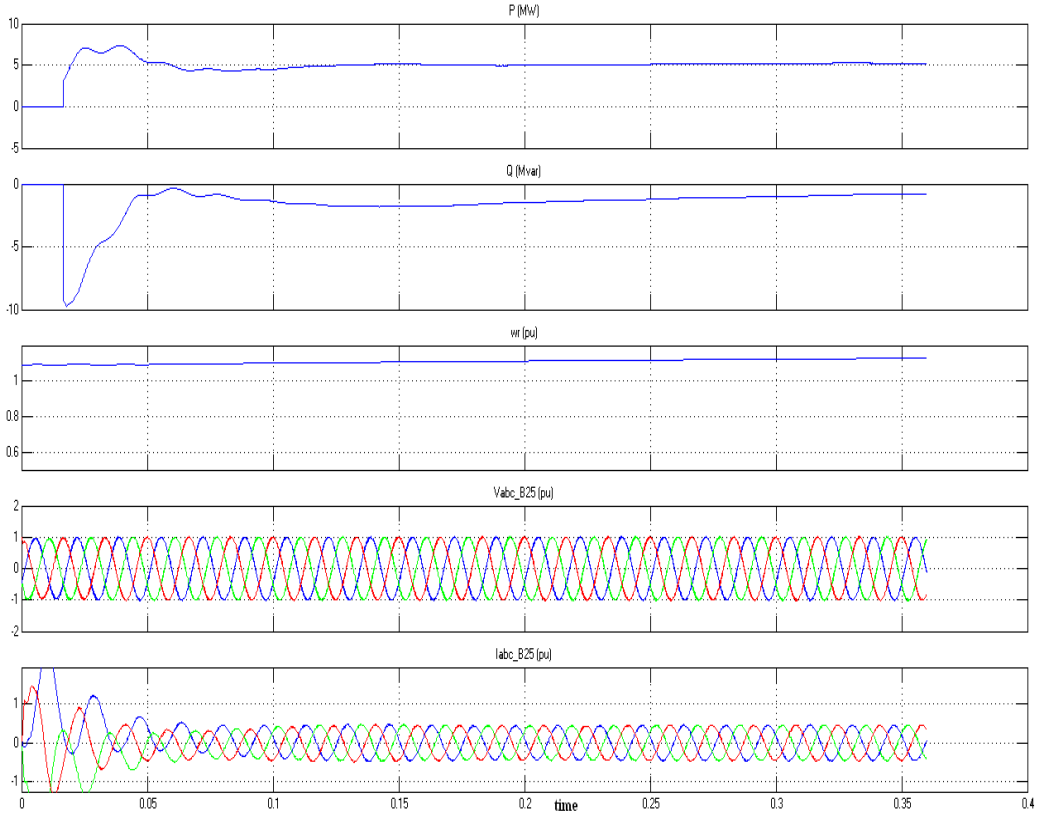

Fig.5.29 Wind Farm not connected with HVDC System

(i) EFFECT OF CHANGE IN BASE WIND SPEED

The mechanical output power of turbine changes with the change in base wind speed. The performance is observed at wind speed 8m/s and 12m/s as shown in Fig. 30(a), (b) respectively. It is observed at 8m/s the active power reduces to 4MW, which is less as compared to nominal power observed in Fig. 5.29. Similarly, at 12m/s the active power increases to 8MW.

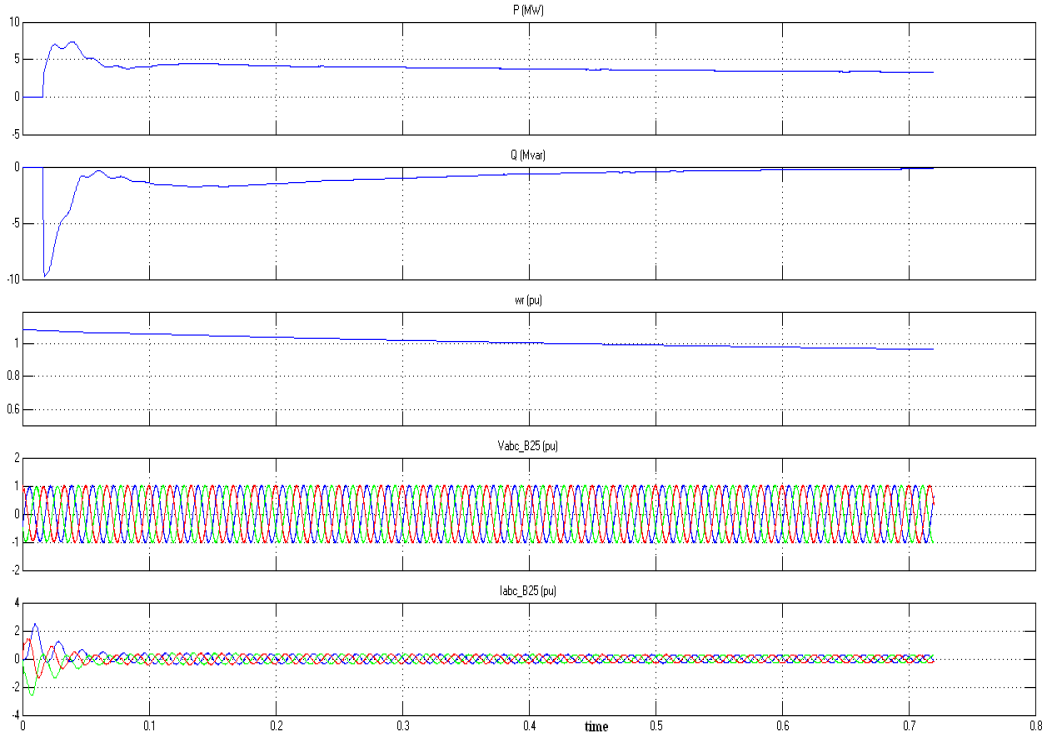

Fig.5.30 (a) Effect of wind speed 8m/s

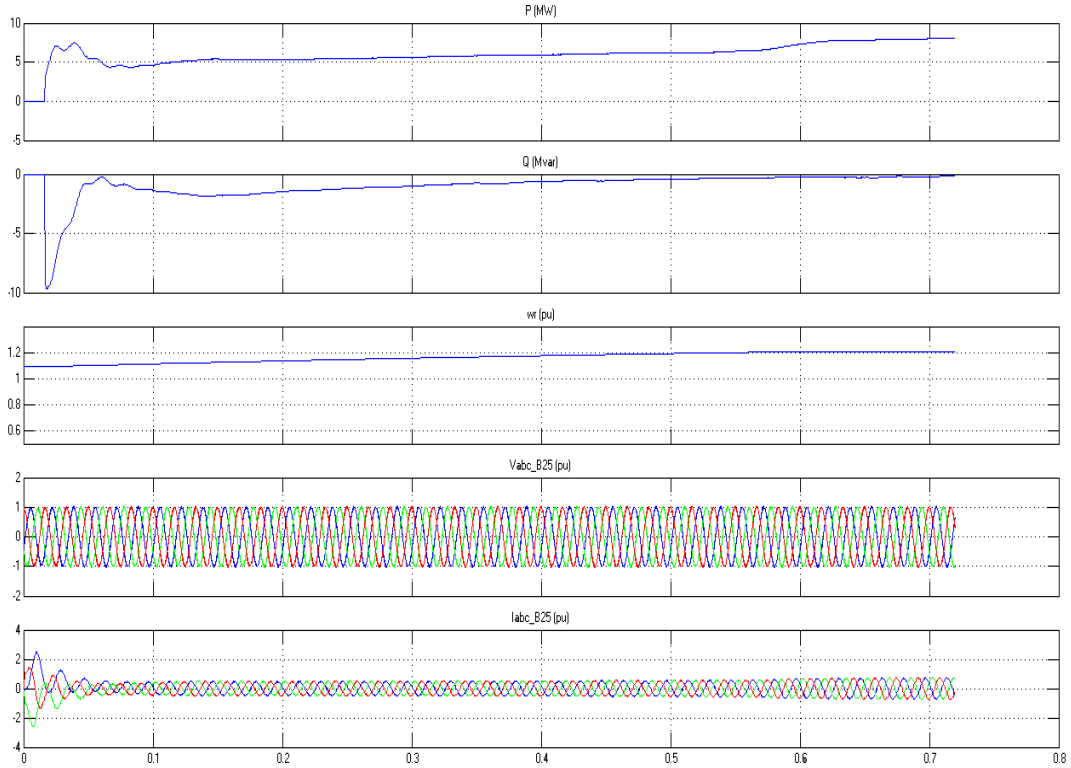

Fig.5.30 (b) Effect of wind speed 12m/s

(ii) EFFECT OF CHANGE IN AC PARAMETER

The change in transmission line parameter is studied by changing the transmission line length. The performance is studied for 10km and 80km line length and results are shown in Fig.5.31(a),(b).A transient in AC busB25 current for the distance of 10km (3.5pu) is higher as compared with the distance of 80 km (1.5pu), as the settling time is greater. The momentarily demand of reactive power is high for short length line as compared to long length line. These values are 15 pu and 5 pu as shown in Fig.5.31 (a),(b). The short line is characterized by small inductance and thus also results into high amplitude transients in current.

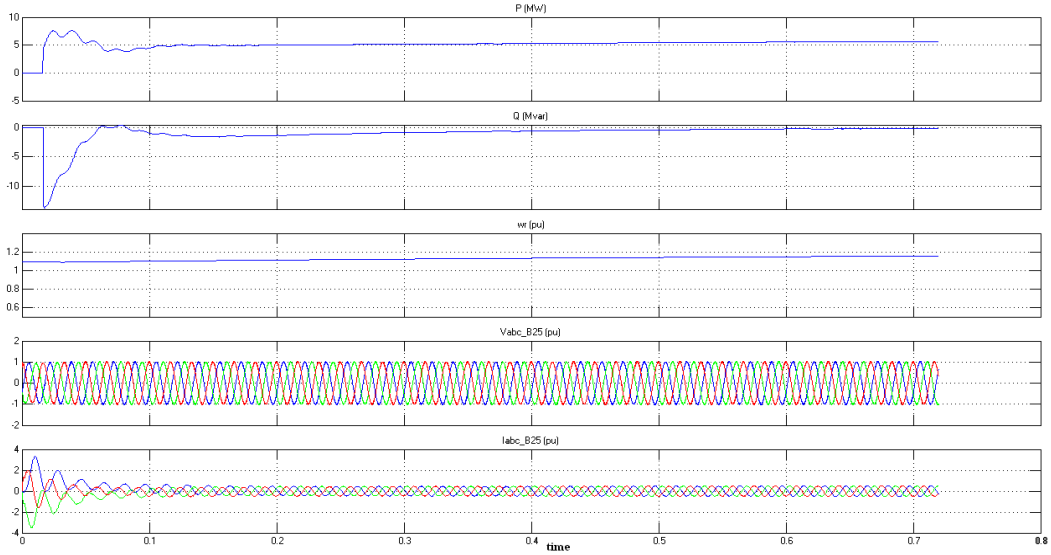

Fig.5.31 (a) Effect of 10km Line

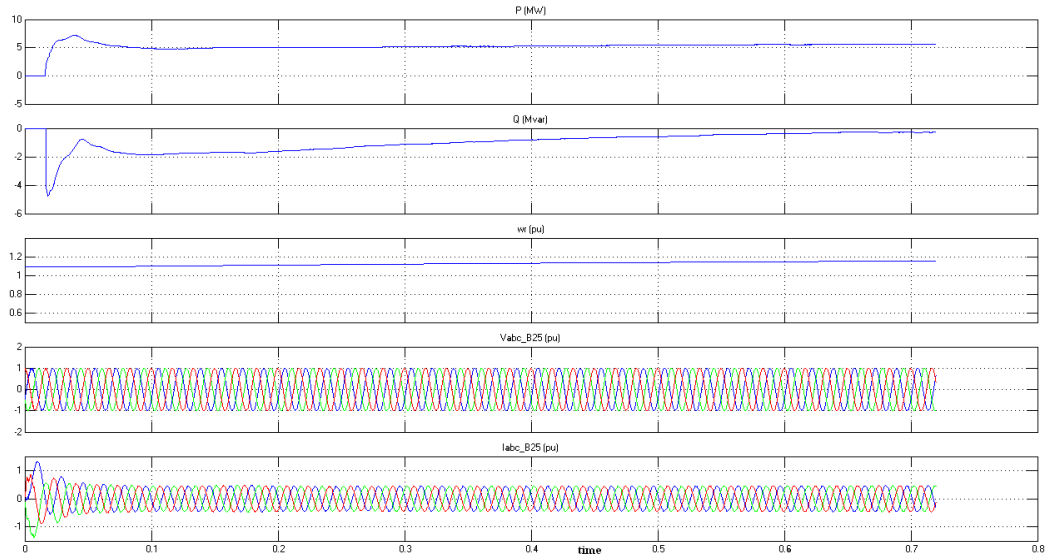

Fig.5.31 (b) Effect of 80km Line

(iii) EFFECT OF CHANGE IN GRID VOLTAGE

On changing the grid voltage to ± 10%, the waveforms observed are as shown in Fig. 32 (a), (b). Thus, the change in reactive power and current is experienced, while real power remains largely unchanged. For higher voltage, reactive demand is slightly more.

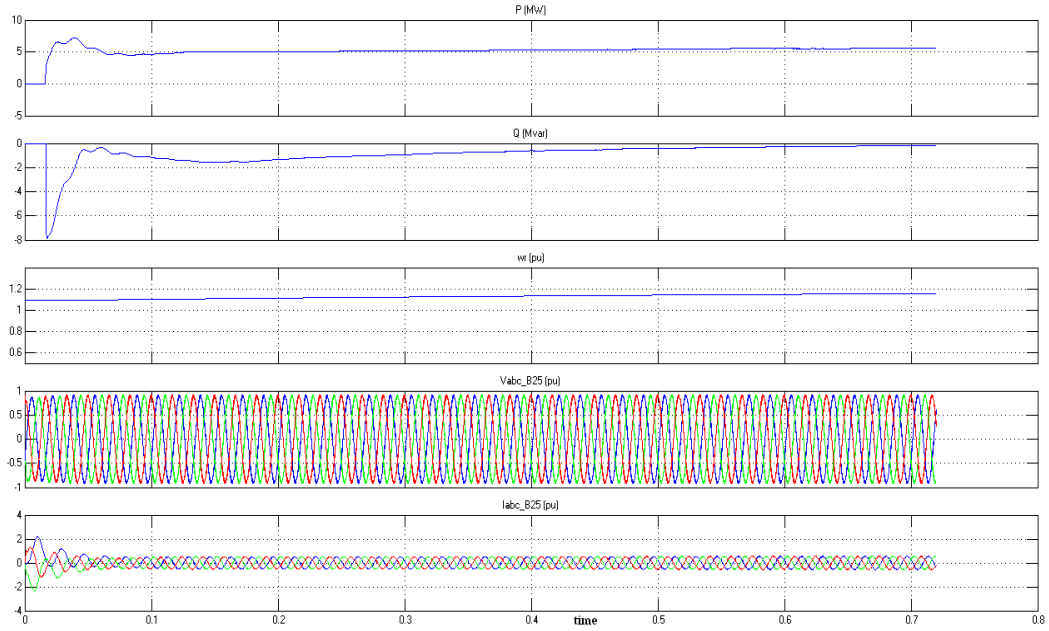

Fig.5.32 (a) Effect for 108kV Grid Voltage

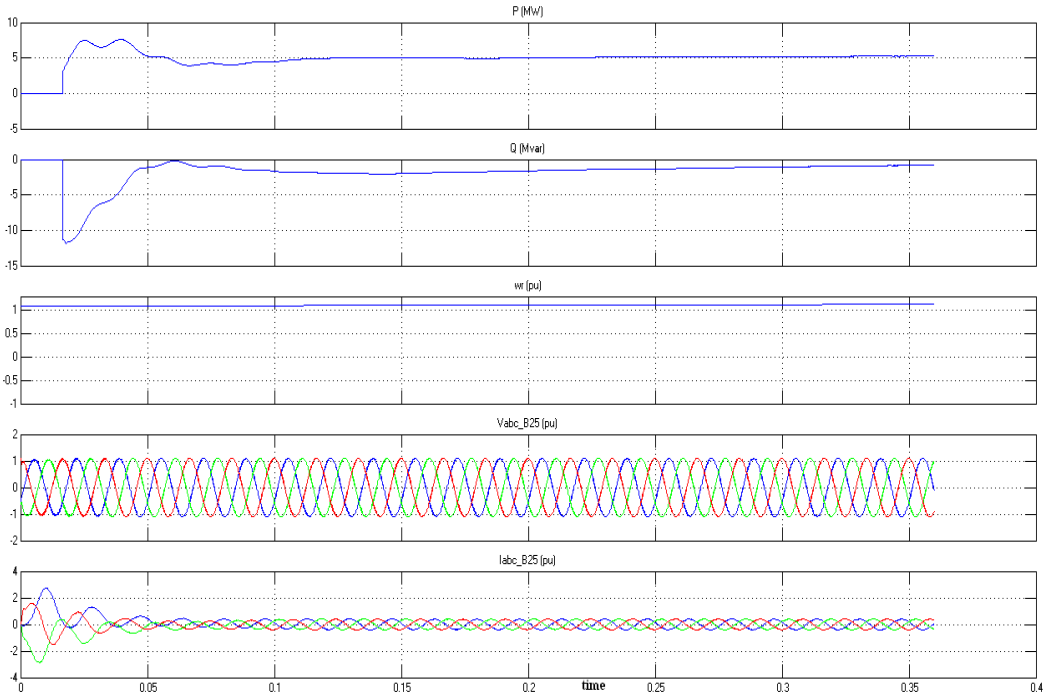

Fig.5.32 (b) Effect for 132kV Grid Voltage

CHAPTER 6
CONCLUSIONS AND FUTURE SCOPE

6.1 CONCLUSIONS

The dynamic performance of wind driven doubly fed induction generator (DFIG) has been studied for two cases: DFIG connected with HVDC transmission system, and DFIG connected without HVDC system. The dynamic models of these systems have been derived in synchronous reference frame and performance has been simulated using MATALB/SIMULINK. The performance has been studied for change in various parameters. The following conclusions are drawn from the study –

- The mechanical output power of the turbine changes with the change in base wind speed.
- With increase in the length of DC transmission line, the voltage drop results into lower voltage at the consumer end resulting into higher losses.
- With the increase in the consumer load, the consumer end voltage decreases.
- The change at consumer end voltage is directly related to change in grid voltage. At higher voltage, reactive power consumed by DFIG is slightly more.
- For lower length of AC transmission line, high amplitude transients in current are resulted.

6.2 SCOPE OF FUTURE WORK

The scope of future work has been identified as-

- Realization of control scheme and tuning of parameters to provide constant voltage during the change of load, line parameters also.
- Investigate the performance with various non-linear loads also.
- Implementation of whole system with bipolar HVDC system instead of monopolar system.

REFERENCES

1. Xiang, D.; Ran, L.; Bumby ,J R.; Tavner, P. J.; Yang, S.; "Coordinated Control of an HVDC Link and Doubly Fed Induction Generators in a Large Offshore Wind Farm", IEEE Transactions On Power Delivery, Vol. 21, No. 1, January 2006.

2. Lu, W.; Ooi, B. T.; "Optimal acquisition and aggregation of offshore wind power by multiterminal voltage-source HVDC", IEEE Transactions On Power Delivery, vol. 18, no. 1, pp. 201–206, Jan. 2003.

3. Pena, R.; Clare, J., Asher,G.; "Doubly fed induction generator using back-to-back converters and its application to variable-speed wind-energy generation," Proceedings of IEEE Power Applications, vol. 143, no. 3, pp. 231–241, 1996.

4. Feltes, C.; Erlich, I.; "Variable frequency operation of DFIG based Wind Farms connected to the grid through VSC-HVDC Link:, Proceedings of IEEE Power Engineering Society, Tampa, Florida, 2007.

5. Muller, S.; Deicke, M.; De Doncker, R. W.; "Doubly fed induction generator systems for wind turbine", IEEE Industrial. Applications Management, vol. 8, no. 3, pp. 26–33, May/Jun. 2002.

6. Søbrink, K.; Sørensen, P.L.; Christensen, P.; Andersen, N.; Eriksson,, K.; Holmberg, P.; "DC Feeder for Connection of a Wind Farm", CIGRE Symposium, Kuala Lumpur, Malaysia, September 1999.

7. Babu, B.C.; Mohanty, K.B.; "Doubly-Fed Induction Generator for Variable Speed Wind Energy Conversion Systems- Modeling & Simulation," International Journal of Computer and Electrical Engineering, Vol. 2, No. 1, February, 2010.

8. Krzeminski, Z.; "Control systems of doubly fed induction machine based on multi-scalar model," in Proceedings of 11thWorld Congress International Federation Automatic Control, pp. 521–526, New York, 1991.

9. Machmoum, M.; Doeuff, R. L.; Sargos, F. M.; "Steady state analysis of a doubly fed asynchronous machine supplied by a current controlled cycloconverter in the rotor," Proceedings of IEE, Vol. 139, No. 2, pp. 114–122, 1992.

10. Rodriguez, J.; Fernandez, J. L.; Beato, D.; "Incidence on power system dynamics of high penetration of fixed speed and doubly fed wind energy systems: study of the Spanish case," IEEE Transactions Power System, Vol. 17, No. 4, pp. 1089–1095, November. 2002.

11. Ye, Fei; Huang, Xueliang; Wang, C.; Zhou, G.; Luo, P.; "The Impact and Simulation on Large Wind Farm Connected to Power System," DRPT2008, Nanjing, China, 6-9 April 2008.

12. Arrillaga, J.; "High Voltage Direct Current Transmission," series IEE Power and Energy Series 29, pp. 10–55, London, U.K., IEE, 1998.

13. Kirby, N. M.; Xu, L.; Luckett, M.; Siepmann, W.; "HVDC transmission for large offshore wind farms," IEE Power Engineering, Journal, Vol.16, No.3, pp. 135–141, 2002.

14. Ekanayake, J. B.; Holdsworth, Lee; Wu, XueGuang; and Jenkins, Nicholas; "Dynamic Modeling of Doubly Fed Induction Generator Wind Turbines," IEEE Transactions On Power Systems, Vol. 18, No. 2, May 2003.

15. Tapia, A.; Tapia, G.; Ostolaza, J. X.; Sáenz, J. R.; "Modeling and Control of a Wind Turbine Driven Doubly Fed Induction Generator", IEEE Transactions on Energy Conversion, Vol. 18, No. 2, June 2003.

16. Salman, S.K.; Badrzadeh, B.; "New approach for modeling doubly fed induction generator (DFIG) for grid connection studies", pp: 1-13. www.2004ewec.info.

17. Das, M.K.; Chowdhury, S.; Gaunt, C.T.; Chowdhury, S.P.;" Control of a Grid Connected Doubly-Fed Induction Generators for Wind Energy Conversion", Proceedings of 44th International Power Engineering, pp 1-5, Glasgow, Scotland, 2009.

18. Lei, Y.; Mullane, A.; Lightbody, G.; Yacamini, R.; "Modeling of the Wind Turbine with a Doubly Fed Induction Generator for Grid Integration Studies", IEEE Transactions on Energy Conversion, Vol. 21, No. 1, March 2006.

19. Aktarujjaman, M.; Haque, M.E.; Muttaqi, K.M.; Negnevitsky, M.; Ledwich, G.; "Control Dynamics of a DFIG under sub- and super-synchronous modes of operation", Proceedings of IEEE Power and Energy, Pittsburgh, USA, July 2008.

20. Spahic, E.; Balzer, G.; "Control Possibility for Offshore Wind Farms," 15th PSCC, Liege, Session 33, Paper 3, Page 1-7, 22-26 August 2005.

21. Neris, A.; Vovos, N.; Giannakopaulos, G.; "A variable speed wind energy conversion scheme for connection to weak ac systems," IEEE Transactions on Energy Conversion, Vol. 14, No. 1, pp. 122–127, Mar. 1999.

22. Mauricio, J.M.; Exposito, A.G.; "Modeling and Control of an HVDC-VSC Transmission System," Transmission & Distribution Conference and Exposition, TDC '06. IEEE/PES, Caracas, Latin America, 15-18 Aug. 2006.

APPENDIX

Parameters	Values
Number Of Units of 1.5MW Wind Farm	6
ASYNCHRONOUS MACHINE DATA	
Nominal power (VA), Pnom	1.5e6/0.9*6
Line-Line voltage (Vrms), Vnom	575
Nominal Frequency, Fnom	60 Hz
Stator Resistance, Rs	0.00706 pu
Stator Inductance, Lls	0.171 pu
Rotor Resistance, Rr	0.005 pu
Rotor Inductance, Llr	0.156 pu
Mutual Inductance, Lm	2.9 pu
Inertia constant ,H	5.04
Friction factor (pu), F	0.01
Number of pairs of poles, p	3
CONTROL SYSTEM OF BOTH SIDE CONVERTERS	
PWM Frequency	27*Fnom
Nominal DC Voltage	1200 Volts
Capacitance of DC link	10000e-6*6 F
R_RL	0.30/100 pu
L_RL	0.30 pu
Nominal power (W), Pmec	1.5e6*6
Power_C	0.73 pu
Speed_A	0.7 pu
Speed_B	0.71pu
Speed_C	1.21pu
Speed_D	1.21pu
Converter Maximum Power	0.5pu
Pitch angle controller gain	500
Maximum pitch angle	45^0
Reactive power regulator gains Kp, Ki	0.05,5
DC bus regulator gains Kp, Ki	0.002,0.05

Grid side converter current regulator gains Kp,Ki	2.5,500
Rotor side converter current regulator gains Kp,Ki	0.3,8
HVDC SYSTEM	
TRANSFORMER	
Nominal Power	5MVA
Frequency	50Hz
R1(pu)	0.004
L1(pu)	0.02
R2(pu)	0.004
L2(pu)	0.02
RECTIFIER	
Snubber Resistance Rs	100ohms
Capacitance Cs	0.1uF
Forward Voltage	0.8V
DC LINE	
Resistance, R	0.015ohm
Inductance ,L	0.2uH
Capacitance, C	0.004uF
Length of Line	200km
PWM INVERTER	
Snubber Resistance Rs	3000ohms
Resistance, Ron	10^{-3}
LC FILTERS	
Inductance, L	2mH
Capacitance, C	3kvar
RLC LOAD	
Active Power, P	500W
Inductive Power, QL	10var
Reactive Power, QC	30kvar